Table 1 Five-year survival rates for predictive variables in patients with hypertrophic cardiomyopathy in Japan

	n (%)	Deaths	5-year survival rate	p Value for log rank test
Sex				
Men	1118 (69.7)	142	0.87	
Women	487 (30.3)	85	0.84	0.151
Age (years)				
<30	157 (9.9)	14	0.90	
30–59	531 (33.1)	42	0.92	
≥60	917 (57.1)	158	0.82	<0.001
BMI (kg/m^2)				
<20	182 (14.0)	40	0.77	
20–24.9	733 (56.3)	92	0.87	
≥25	387 (29.7)	39	0.90	<0.001
Family history of HCM				
Yes	207 (16.9)	27	0.87	
No	1015 (83.1)	132	0.87	0.991
Hypertension				
Yes	456 (31.2)	68	0.85	
No	1005 (68.8)	129	0.87	0.336
Diabetes mellitus				
Yes	131 (8.9)	30	0.76	
No	1332 (91.1)	178	0.86	0.002
Alcohol drinking				
Yes	475 (36.3)	71	0.85	
No	832 (63.7)	113	0.86	0.525
Smoking				
Yes	535 (39.3)	68	0.87	
No	825 (60.7)	115	0.86	0.524
NYHA classification				
I	908 (65.3)	89	0.90	
II	406 (29.2)	62	0.84	
III	62 (4.5)	28	0.53	
IV	14 (1.0)	7	0.43	<0.001
Rhythm				
Sinus rhythm	1347 (91.4)	161	0.88	
Atrial fibrillation	113 (7.7)	28	0.74	
Atrial flutter	13 (0.9)	4	0.68	<0.001
Left ventricular hypertrophy (detected by ECG)				
Yes	1021 (68.9)	132	0.86	
No	461 (31.1)	61	0.87	0.814
LBBB				
Yes	45 (3.3)	15	0.66	
No	1303 (96.7)	165	0.87	<0.001
Apical hypertrophy				
Yes	532 (41.1)	56	0.89	
No	763 (58.9)	110	0.85	0.031
CTR (%)				
<50	353 (26.7)	25	0.93	
50–54	484 (36.7)	54	0.89	
55–59	283 (21.4)	36	0.87	
≥60	200 (15.2)	59	0.70	<0.001
LVEF (%)				
<50	67 (5.9)	27	0.59	
50–59	88 (7.8)	19	0.77	
60–69	243 (21.5)	29	0.88	
70–79	439 (38.9)	49	0.89	
≥80	292 (25.9)	31	0.89	<0.001
Thickness of IVS (mm)				
<11	145 (9.8)	17	0.88	
11–15	540 (36.5)	62	0.88	
16–20	476 (32.1)	68	0.85	
21–25	208 (14.0)	37	0.83	
≥26	112 (7.6)	18	0.83	0.255
Hospital beds				
<299	140 (8.9)	27	0.79	
300–399	93 (5.9)	19	0.80	
400–499	121 (7.7)	14	0.88	
≥500	360 (22.8)	60	0.83	
University hospital	867 (54.8)	93	0.89	0.002
Time from diagnosis (years)				
<1	463 (30.6)	62	0.86	
1–1.9	116 (7.7)	16	0.85	
2–2.9	144 (9.5)	15	0.89	
3–3.9	97 (6.4)	14	0.85	
4–4.9	97 (6.4)	14	0.85	
5–9.9	312 (20.6)	35	0.89	
≥10	283 (18.7)	51	0.81	0.231

BMI, body mass index; CTR, cardiothoracic ratio; HCM, hypertrophic cardiomyopathy; IVS, interventricular septum; LBBB, left bundle branch block; LVEF, left ventricular ejection fraction; NYHA, New York Heart Association.

Table 2 Multivariate-adjusted HRs of predictive variables for all-cause mortality in patients with hypertrophic cardiomyopathy

	Adjusted HR* (95% CI)	Wald statistic	p Value
Sex			
Men	1		
Women	0.77 (0.46 to 1.30)	1	0.324
Age			
1-year increase	1.02 (1.01 to 1.04)	8.2	0.004
Diabetes mellitus			
Yes	1.03 (0.47 to 2.28)	<0.1	0.941
No	1		
NYHA classification			
I	1		
II	1.19 (0.74 to 1.94)	0.5	0.472
III	3.41 (1.75 to 6.67)	12.9	<0.001
IV	2.85 (0.87 to 9.39)	3.0	0.084
Rhythm			
Sinus rhythm	1		
Atrial fibrillation	1.36 (0.75 to 2.46)	1.0	0.306
Atrial flutter	0.62 (0.16 to 2.30)	0.5	0.471
LBBB			
Yes	3.14 (1.28 to 7.71)	6.2	0.013
No	1		
Apical hypertrophy			
Yes	0.58 (0.36 to 0.92)	5.4	0.021
No	1		
CTR† (increase of 6.2%)	1.61 (1.26 to 2.05)	14.4	<0.001
BMI† (increase of 3.4 kg/m^2)	0.80 (0.63 to 1.01)	3.7	0.056
Thickness of IVS† (increase of 5.8 mm)	1.15 (0.94 to 1.40)	1.9	0.163
LVEF (decrease of 13%)	1.42 (1.20 to 1.69)	16.4	<0.001

BMI, body mass index; CTR, cardiothoracic ratio; IVS, interventricular septum; LBBB, left bundle branch block; LVEF, left ventricular ejection fraction; NYHA, New York Heart Association.
*All variables are included in the same model.
†Hazard ratio for 1 SD increase or decrease; value of 1 SD given in parentheses.

DISCUSSION

In this paper, we report the crude probability of death and the HRs for all-cause mortality by baseline prognostic factors, from a nationwide study of HCM in Japan. To our knowledge, this is the first nationwide follow-up survey in Japan conducted on patients with HCM.

One methodological issue in this survey involves the diagnostic criteria used. In 1995, the World Health Organization/International Society and Federation of Cardiology task force reported a new definition and classification of cardiomyopathy in which the cardiomyopathies were defined simply as diseases of the myocardium associated with cardiac dysfunction.[11] However, we used the definition and classification provided by the earlier task force of 1980,[9 10] in which idiopathic cardiomyopathy was distinguished from other specific heart muscle diseases. Our reasons for doing this were, firstly, that nearly all cardiologists and specialists in general medicine in Japan have been applying this definition to their diagnosis of cardiomyopathies for a long time; and secondly, that numerous previous reports have also used the same definition, allowing us to compare our data with those reports.

General clinical outcome

Several previous clinical studies on the natural history and prognosis of HCM have been based on populations of selected patients from referral centres,[12-14] and therefore, on the basis of different levels of care and management, various prognoses would be expected. The clinical outcome and perception of prognostic factors in HCM is profoundly affected by a bias in patient selection.[15] However, our study is free from this referral bias since patients were recruited from all over the nation and from different diagnostic centres.

The average (SD) age at entry into study was 58.0 (17.5) years. Both the overall crude probability of 5-year survival in our study (86%) and the annual mortality (2.2–3.0%) were comparable with the results from Western studies,[14 16] which were based on selected referral centres. According to previous report,[8] the male/female ratio for HCM is 2:3 in Japan. In our study, the probability of survival did not differ between women and men, a finding which is consistent with previous data on sex comparisons of survival in patients with HCM.[16] However, in Chinese patients, HCM was found to have a worse clinical outcome in female patients.[13] The reason for this inconsistency between our data and Chinese patients is not clear, but the small number of participants in the Chinese study and the point that less female than male patients were in the stage I of the NYHA function class in their study may explain the difference with our result.

Prognostic factors

Our results suggest for the first time that a simple chest *x* ray could be a reliable prognostic predictor in HCM. Although a CTR of 55–59% (21.4% of study patients) posed a slight increase in the risk of mortality, a CTR of >60% (15.2% of study patients) was strongly associated with a poorer prognosis. LVEF at baseline was also found to be a significant predictor of all-cause mortality in our study, with an LVEF of <60% (13.7% of study patients) associated with poorer prognosis. Progression of HCM to LV dilatation and systolic dysfunction sometimes occurs, although the mechanism of this is not fully understood.[17] However, data are limited on the prognosis of different LVEF levels in patients with HCM. Our findings confirmed the result of a previous study involving 10 patients with HCM, which concluded that an LVEF of <50% was associated with poor prognosis.[18]

Apical hypertrophy has been associated with a more benign prognosis and rarely with cardiovascular mortality and morbidity in Western populations of patients with HCM.[19 20] Our data support this finding, as patients with apical hypertrophy had a better prognosis in the multivariate model. Previous studies in the Japanese population have also indicated a benign prognosis in patients with this condition.[21 22]

A direct relationship between LV wall thickness and the risk of sudden death or heart failure-related death has been reported in patients with HCM.[23-25] Our data did not support this finding, as LV wall thickness did not show a significant relationship with prognosis. Our results support previous findings that suggest LV wall thickness should not be considered as an isolated risk factor for mortality due to cardiovascular diseases in patients with HCM.[26 27] Olivotto *et al*[27] proposed that the presence of LV hypertrophy might be a potential risk factor for sudden death only in those patients diagnosed with HCM at a very young age.

In a community-based HCM study, AF was reported to be a substantial risk factor for heart failure-related mortality and severe functional disability.[28] The prevalence of AF was lower (7.7% of study patients) in our study than the 22% seen in this previous report.[28] In our study, the crude survival rate for all-cause mortality in patients with AF at baseline was significantly lower than for those patients with sinus rhythm. However, the significant relationship with AF disappeared in the multivariate model. We observed that the presence of LBBB at baseline was associated with a poorer prognosis on multivariate analysis. The infrequent occurrence of LBBB in our study (3.3%) was comparable with previous data, which showed a prevalence of 6% among 204 patients with obstructive HCM and free from obstructive coronary artery disease.[29]

Study limitations

Although the follow-up time in our study was limited to 5 years, shorter than follow-up times in previous studies,[13 20 27] our study group was an average of 10 times larger than that of those studies, thus covering a comparable number of patient-years for the subgroups of baseline prognostic factors. A limitation of this study, which is shared by other studies,[13 26] is that a single measurement of prognostic factors, although reproducible and practical for clinical purposes, does not accurately reflect the total burden of predictors in individual patients. Another limitation of this study is that we failed to differentiate HCM-related deaths including sudden deaths and deaths caused by end-stage cardiac failure from other causes of mortality, and we reported all-cause mortality as our main outcome.

CONCLUSIONS

HCM has relatively good prognosis in Japanese patients. A poorer prognosis in HCM is predicted by high cardiothoracic ratio, low LVEF and the presence of LBBB, with a better prognosis in patients with apical hypertrophy. The presence of hypertension, AF and the level of IVS thickness were not independent predictors of prognosis during the 5-year follow-up period.

This study was supported by a grant-in-aid for the Epidemiology of Intractable Diseases Research Committee and a grant-in-aid for Idiopathic Cardiomyopathy Research Committee from the Ministry of Health and Welfare of Japan.

Authors' affiliations

Ali Nasermoaddeli, Katsuyuki Miura, Yoshiyuki Soyama, Yuko Morikawa, Hideaki Nakagawa, Department of Epidemiology and Public Health, Kanazawa Medical University, Ishikawa, Japan
Akira Matsumori, Department of Cardiovascular Medicine, Kyoto University Graduate School of Medicine, Kyoto, Japan
Akira Kitabatake, Department of Cardiovascular Medicine, Hokkaido University Graduate School of Medicine, Sapporo, Japan
Yutaka Inaba, Department of Epidemiology and Environmental Health, Juntendo University School of Medicine, Tokyo, Japan

Competing interests: None declared.

We disclose that there are no other financial, personal or professional relationships with other people or organisations that could be perceived as conflicts of interest, or as potentially influencing or biasing this work.

REFERENCES

1 **Maron BJ.** Hypertrophic cardiomyopathy: a systematic review. *JAMA* 2005;**287**:1308–20.
2 **Maron BJ.** Hypertrophic cardiomyopathy. *Lancet* 1997;**350**:127–33.
3 **Spirito P,** Seidman CE, Mckenna WJ, *et al.* Management of hypertrophic cardiomyopathy. *N Engl J Med* 1997;**30**:775–85.
4 **Wigle ED,** Rakowski H, Kimball BP, *et al.* Hypertrophic cardiomyopathy: clinical spectrum and treatment. *Circulation* 1995;**92**:1680–92.
5 **Louie EK,** Edwards LC. Hypertrophic cardiomyopathy. *Prog Cardiovasc Dis* 1994;**36**:275–308.
6 **Maron BJ.** Hypertrophic cardiomyopathy: an important global disease. *Am J Med* 2004;**116**:63–6.
7 **Matsumori A,** Furukawa Y, Hasegawa K, *et al.* Epidemiological and clinical characteristics of cardiomyopathies in Japan: results from nationwide surveys. *Circ J* 2002;**66**:323–36.
8 **Miura K,** Nakagawa H, Morikawa Y, *et al.* Epidemiology of idiopathic cardiomyopathy in Japan: results from a nationwide survey. *Heart* 2002;**87**:126–30.
9 **The WHO/ISFC task force on the definition and classification of cardiomyopathies.** Report of the WHO/ISFC task force on the definition and classification of cardiomyopathies. *Br Heart J* 1980;**44**:672–3.
10 **Research committee on idiopathic cardiomyopathy.** Guidelines for the diagnosis of idiopathic cardiomyopathy. In: Annual report of the research committee on idiopathic cardiomyopathy (in Japanese). Tokyo: Ministry of Health and Welfare, Japan, 1985:13–15.
11 **Richardson P,** Mckenna W, Bristow M, *et al.* Report of the 1995 World Health Organization/International Society and Federation of Cardiology Task Force on the definition and classification of cardiomyopathies. *Circulation* 1996;**93**:841–2.
12 **Takagi E,** Yamakado T, Nakano T. Prognosis of completely asymptomatic adult patients with hypertrophic cardiomyopathy. *J Am Coll Cardiol* 1999;**33**:206–11.
13 **Ho HH,** Lee KL, Lau CP, *et al.* Clinical characteristics of long-term outcome in Chinese patients with hypertrophic cardiomyopathy. *Am J Med* 2004;**116**:19–23.
14 **Maron BJ,** Casey SA, Hauser RG, *et al.* Clinical course of hypertrophic cardiomyopathy with survival to advanced age. *J Am Coll Cardiol* 2003;**42**:882–8.
15 **Maron BJ,** Spirito P. Impact of patient selection biases on the perception of hypertrophic cardiomyopathy and its natural history. *Am J Cardiol* 1993;**72**:970–2.
16 **Dimitrow PP,** Czarnecka D, Kawecka-Jaszcz k, et al. Sex-based comparison of survival in referred patients with hypertrophic cardiomyopathy. *Am J Med* 2004;**117**:65–6.
17 **Nakamura K,** Kusano KF, Matsubara H, *et al.* Relationship between oxidative stress and systolic dysfunction in patients with hypertrophic cardiomyopathy. *J Card Fail* 2005;**11**:117–23.
18 **Doi K,** Toda G, Iliev II, *et al.* Clinical analysis of hypertrophic cardiomyopathy which evolved into dilated phase during long-term follow-up. *Jpn Heart J* 1999;**40**:579–87.
19 **Webb JG,** Sasson Z, Rakowski H, *et al.* Apical hypertrophic cardiomyopathy: clinical follow-up and diagnosis correlates. *J Am Coll Cardiol* 1990;**15**:83–90.
20 **Eriksson MJ,** Sonnenberg B, Woo A, *et al.* Long term outcome in patients with apical hypertrophic cardiomyopathy. *J Am Coll Cardiol* 2002;**39**:638–45.
21 **Sakamoto T,** Amano K, Hada Y, *et al.* Asymmetric apical hypertrophy: ten years experience. *Postgrad Med J* 1986;**62**:567–70.
22 **Sakamoto T,** Suzuki J. Apical hypertrophic cardiomyopathy. *Nippon Rinsho* 2000;**58**:93–101.
23 **Maron BJ,** Casey SA, Poliac LC, *et al.* Clinical course and prognosis of hypertrophic cardiomyopathy in a general United States cohort. *JAMA* 1999;**281**:650–5.
24 **Spirito P,** Maron BJ. Relation between extent of left ventricular hypertrophy and occurrence of sudden cardiac death in hypertrophic cardiomyopathy. *J Am Coll Cardiol* 1990;**15**:1521–6.
25 **Spirito P,** Bellone P, Harris KM, *et al.* Magnitude of left ventricular hypertrophy and risk of sudden death in hypertrophic cardiomyopathy. *N Engl J Med* 2000;**342**:1778–85.
26 **Elliott PM,** Gimeno-Blanes JR, Mahon NG, *et al.* Relation between severity of left-ventricular hypertrophy and prognosis in patients with hypertrophic cardiomyopathy. *Lancet* 2001;**357**:420–4.
27 **Olivotto I,** Gistri R, Petrone P, *et al.* Maximum left ventricular thickness and risk of sudden death in patients with hypertrophic cardiomyopathy. *J Am Coll Cardiol* 2003;**41**:315–21.
28 **Olivotto I,** Cecchi F, CaseySA, et al. Impact of atrial fibrillation on the clinical course of hypertrophic cardiomyopathy. *Circulation* 2001;**104**:2517–24.
29 **Qin JX,** Shiota T, Lever HM, *et al.* Conduction system abnormalities in patients with obstructive hypertrophic cardiomyopathy following septal reduction interventions. *Am J Cardiol* 2004;**93**:171–5.

Research article

A cardiac myosin light chain kinase regulates sarcomere assembly in the vertebrate heart

Osamu Seguchi,[1] Seiji Takashima,[2,3] Satoru Yamazaki,[1] Masanori Asakura,[1] Yoshihiro Asano,[2] Yasunori Shintani,[2] Masakatsu Wakeno,[1] Tetsuo Minamino,[2] Hiroya Kondo,[2] Hidehiko Furukawa,[4] Kenji Nakamaru,[4] Asuka Naito,[4] Tomoko Takahashi,[4] Toshiaki Ohtsuka,[4] Koichi Kawakami,[5] Tadashi Isomura,[6] Soichiro Kitamura,[1] Hitonobu Tomoike,[1] Naoki Mochizuki,[1] and Masafumi Kitakaze[1]

[1]Department of Cardiovascular Medicine, National Cardiovascular Center, Suita, Osaka, Japan. [2]Department of Cardiovascular Medicine and [3]Health Care Center, Osaka University Graduate School of Medicine, Suita, Osaka, Japan. [4]Core Technology Research Laboratories, Sankyo Co. Ltd., Shinagawa, Tokyo, Japan. [5]Division of Molecular and Developmental Biology, National Institute of Genetics, Mishima, Shizuoka, Japan. [6]Hayama Heart Center, Hayama, Kanagawa, Japan.

Marked sarcomere disorganization is a well-documented characteristic of cardiomyocytes in the failing human myocardium. Myosin regulatory light chain 2, ventricular/cardiac muscle isoform (MLC2v), which is involved in the development of human cardiomyopathy, is an important structural protein that affects physiologic cardiac sarcomere formation and heart development. Integrated cDNA expression analysis of failing human myocardia uncovered a novel protein kinase, cardiac-specific myosin light chain kinase (cardiac-MLCK), which acts on MLC2v. Expression levels of cardiac-MLCK were well correlated with the pulmonary arterial pressure of patients with heart failure. In cultured cardiomyocytes, knockdown of cardiac-MLCK by specific siRNAs decreased MLC2v phosphorylation and impaired epinephrine-induced activation of sarcomere reassembly. To further clarify the physiologic roles of cardiac-MLCK in vivo, we cloned the zebrafish ortholog z-cardiac-MLCK. Knockdown of z-cardiac-MLCK expression using morpholino antisense oligonucleotides resulted in dilated cardiac ventricles and immature sarcomere structures. These results suggest a significant role for cardiac-MLCK in cardiogenesis.

Introduction

Despite recent advances in pharmacologic and surgical therapies, chronic heart failure (CHF) is still a leading cause of death worldwide (1). Currently, heart transplant is thought to be the most effective therapy for end-stage CHF. However, this approach obviously cannot be used for all of the numerous affected patients and is not suitable for patients with a mild disease state. Therefore, there is increasing demand for new therapeutic targets for CHF.

Cardiomyocytes, the most basic cellular unit of the myocardium, express several sarcomeric proteins, including myosin and actin; abnormalities in these sarcomeric proteins are major causes of idiopathic cardiomyopathies and lead to CHF (2–4). Type II myosin is the major constituent of sarcomeres. In the neck region of this protein, there are binding sites for a pair of myosin light chains, which are called the essential light chain and the regulatory light chain. Among the several paralogs of the myosin regulatory light chain in vertebrates (5), myosin regulatory light chain 2, ventricular/cardiac muscle isoform (MLC2v) is expressed in the myocardium, where it performs specific roles in cardiogenesis by contributing to the formation of sarcomeres and in increasing the Ca^{2+} sensitivity of muscle tension at submaximal Ca^{2+} concentrations (6, 7). Currently, 2 members of the myosin light chain kinase (MLCK) protein family that act on myosin regulatory light chain in muscle cells have been identified, skeletal muscle MLCK (skMLCK) and smooth muscle MLCK (smMLCK) (8). Among these MLCK family members, smMLCK, including nonmuscle isoforms, is distributed ubiquitously in various tissues and contributes to the contraction of smooth muscle and several cell activities. Conversely, skMLCK is thought to localize and function in both cardiac muscle and skeletal muscle (9); to our knowledge, no cardiac-specific MLCK has been reported to date. skMLCK-deficient mice, however, did not show any heart weight, body weight, or heart weight/body weight ratio phenotypes, despite effective knockdown of skMLCK expression (10). Additionally, there were no significant differences between the knockout and wild-type animals in regard to MLC2v phosphorylation, suggesting the existence of as-yet unknown kinases in cardiac muscle cells.

Genome-wide analyses, which have recently become available in a wide range of clinical settings, such as cancer research, allow for a global view of gene expression in certain disease states and the identification of unknown molecules and molecular pathways that can be exploited as novel therapeutic targets. CHF is a candidate disease for this type of genome-wide analysis, because of its heterogeneous properties and previous difficulties identifying responsible genes using other conventional modalities.

In this study, we performed microarray analysis of the failing human myocardium and examined the correlation between the obtained genomic data and the clinical, physiological, and biochemical characteristics of CHF. In this manner, we sought to identify candidate genes that are involved in the pathophysiology of CHF. Consequently, we identified what we believe to be a novel

Nonstandard abbreviations used: ANP, atrial natriuretic peptide; BNP, brain natriuretic peptide; CHF, chronic heart failure; cardiac-MLCK, cardiac-specific MLCK; Dd, end-diastolic dimension; Ds, end-systolic dimension; FS, fractional shortening; hpf, hours postfertilization; MI, myocardial infarction; MLC2v, myosin regulatory light chain 2, ventricular/cardiac muscle isoform; MLCK, myosin light chain kinase; M-mode, motion mode; MO, morpholino antisense oligonucleotide; p-s15MLC, antibodies for phosphorylated MLC2v; PAP, pulmonary arterial pressure; RcMK, antibodies specific for rodent cardiac-MLCK; si-cMK, siRNA targeting cardiac-MLCK; si-smMK, siRNA targeting rat smMLCK; skMLCK, skeletal muscle MLCK; smMLCK, smooth muscle MLCK; tMLC, antibodies for total MLC2v; z-, zebrafish; z-cMKaugMO, MO targeting the AUG translational start site of z-cardiac-MLCK.

Conflict of interest: The authors have declared that no conflict of interest exists.

Citation for this article: *J. Clin. Invest.* **117**:2812–2824 (2007). doi:10.1172/JCI30804.

Table 1
Clinical characteristics of the patients used for microarray analysis

Pt	Age (yr)	Sex	Diagnosis	Operation	Dd (mm)	EF (%)	PAP (mmHg)	ANP (pg/ml)	BNP (pg/ml)
1	53	M	DCM, MI	Batista	88	25	20	25	90.4
2	45	M	DCM	Batista	81	39	45	85	217
3	72	M	DCM	Batista	71	14	25	86	201
4	58	M	MI	Dor	76	–	–	–	–
5	57	M	HCM, MI	Dor	52	44	41	20	80.3
6	69	M	DCM	Batista	86	19	59	100	465
7	40	M	AR	Unknown	76	42	16	52	271
8	75	M	MI	Dor	51	55	–	39	174
9	32	M	DCM	Batista	81	26	26	300	869
10	51	F	Sarcoidosis	Dor	68	35	–	89	339
11	54	M	MI	Dor	63	37	–	84	302
12	58	M	Myocarditis	Dor	77	22	–	800	2,710
N-1	27	M	Normal	–	–	–	–	–	–
N-2	24	M	Normal	–	–	–	–	–	–

AR, aortic regurgitation; DCM, dilated cardiomyopathy; EF, ejection fraction; F, female; HCM, hypertrophic cardiomyopathy; M, male; Pt, patient.

cardiac-specific MLCK (cardiac-MLCK; encoded by *MYLK3*). Phosphorylation of MLC2v by cardiac-MLCK regulated the reassembly of sarcomere structures in cultured neonatal rat cardiomyocytes. Suppression of cardiac-MLCK expression in zebrafish embryos using specific morpholino antisense oligonucleotides (MOs) led to dilation of the cardiac ventricle with incomplete sarcomere formation, suggesting critical roles for cardiac-MLCK in the heart.

Results

Identification of cardiac-MLCK from failing human myocardia using microarray analysis. To identify candidate genes involved in the pathophysiology of CHF, we used an HG-U95 Affymetrix GeneChip to analyze the gene expression profiles of failing myocardial tissues obtained from 12 patients who had undergone cardiac exclusion surgery, such as the Dor or Batista procedures, for end-stage CHF (Table 1). Figure 1A is an overview flowchart for the selection of candidate genes. Compared with those of 2 normal control samples, the expression of 626 probe sets was significantly upregulated in the failing myocardia. Of these, we selected probe sets whose expression levels were positively correlated ($r > 0.7$) with pulmonary arterial pressure (PAP) measurements (129 probe sets) and brain natriuretic peptide (BNP) mRNA levels (194 probe sets). The tissue localization of each selected probe set was then analyzed using the commercially available BioExpress database (Gene Logic Inc.). We selected 10 probe sets, for which the cardiac expression level was at least 10-fold the mean expression level of 24 other tissues, for further analysis. These probe sets represented a set of genes that included atrial natriuretic peptide (ANP), BNP, small muscle protein, and α-actin, all of which are known to be involved in heart failure, cardiac muscle remodeling, and striated muscle function. We calculated the ratios of expression in cardiac muscle to that in skeletal muscle in these probe sets. ANP (36663_at and 73106_s_at), BNP (39215_at), Importin9 (84730_at), and 75678_at exhibited expression levels that were at least 10-fold greater in the heart than in skeletal muscle. Expression levels of 75678_at, for which annotation was not available, were similar to those of ANP and BNP. We hypothesized that this unknown transcript was involved in the pathophysiology of heart failure.

Using 5′-RACE, we identified specific sequences identical to those of NM_182493 (*MYLK3*) located 4 kb upstream of the probe set sequence. The relative expression level of this candidate gene was significantly correlated with the relative PAP value (Figure 1B); in addition, the expression of this gene was restricted to the heart (Figure 1C). A homology search using the transcript sequence, particularly the sequence coding for the C-terminal kinase domain, identified *MYLK3* as a member of the MLCK family. Thus, we named the protein encoded by *MYLK3* "cardiac-MLCK." Two distinct MLCK family genes have been previously reported: *MYLK*, which encodes smMLCK, and *MYLK2*, which encodes skMLCK (8). Domain structure analysis revealed a well-conserved serine/threonine kinase domain that includes an ATP-binding site and an active serine/threonine kinase domain positioned near the C terminus of the cardiac-MLCK protein (Figure 1D). The expression patterns of the MLCK family members were confirmed by Northern blot analysis. As previously described (11), 2 major transcripts of *MYLK* were almost ubiquitously expressed. The larger transcript codes for a nonmuscle isoform of smMLCK generated by alternative splicing. Restricted expression patterns were observed for both *MYLK2* and *MYLK3*. *MYLK2* expression was only detected in skeletal muscle, whereas *MYLK3* expression was only observed in the heart (Figure 1E). *MYLK* was also found to be expressed in the heart, although its expression was not upregulated in failing myocardia as much as the expression of *MYLK3* (data not shown). To assess the physiological significance of cardiac-MLCK, we generated an adenovirus vector encoding cardiac-MLCK. In serum-free conditions, cultured neonatal rat cardiomyocytes showed predominantly disorganized sarcomere structures. Overexpression of cardiac-MLCK in cultured neonatal rat cardiomyocytes augmented sarcomere organization under serum-starved conditions (cells with organized sarcomeres, 28.7% ± 11.1% versus 3.1% ± 2.4%; $P < 0.001$; Figure 1, F and G), suggesting that cardiac-MLCK participates in sarcomere formation in cardiomyocytes.

Cardiac-specific myosin regulatory light chain is a specific substrate of cardiac-MLCK. Because this protein kinase contained a consensus kinase catalytic domain, we attempted to identify potential substrates of cardiac-MLCK. To identify physiological substrates of cardiac-MLCK, we screened murine heart homogenates using an in vitro kinase reaction. After fractionation of murine heart homogenates using a cation exchange column, aliquots of each fraction were subjected to an in vitro kinase reaction with recombinant cardiac-MLCK. Fractions 10 and 11 each contained a distinct 20-kDa band that was labeled with ^{32}P only in the presence of recombinant cardiac-MLCK (Figure 2A). This ^{32}P-labeled 20-kDa protein was purified (Figure 2B) and analyzed using matrix-assisted laser desorption/ionization-time-of-flight mass spectrometry and peptide mass fingerprinting. The 20-kDa protein contained fragments with amino acid sequences that were homologous to murine MLC2v (Figure 2C). No additional ^{32}P-labeled proteins were detected in fractions obtained following cation or anion exchange column purification. Further analysis of this phosphorylation event in vitro revealed endogenous MLC2v, purified from murine heart homogenates, was phosphorylated by recombinant cardiac-MLCK in a Ca^{2+}-calmodulin–dependent manner (Figure 2D). Thus, we conclude that cardiac-MLCK is a calmodulin-dependent kinase.

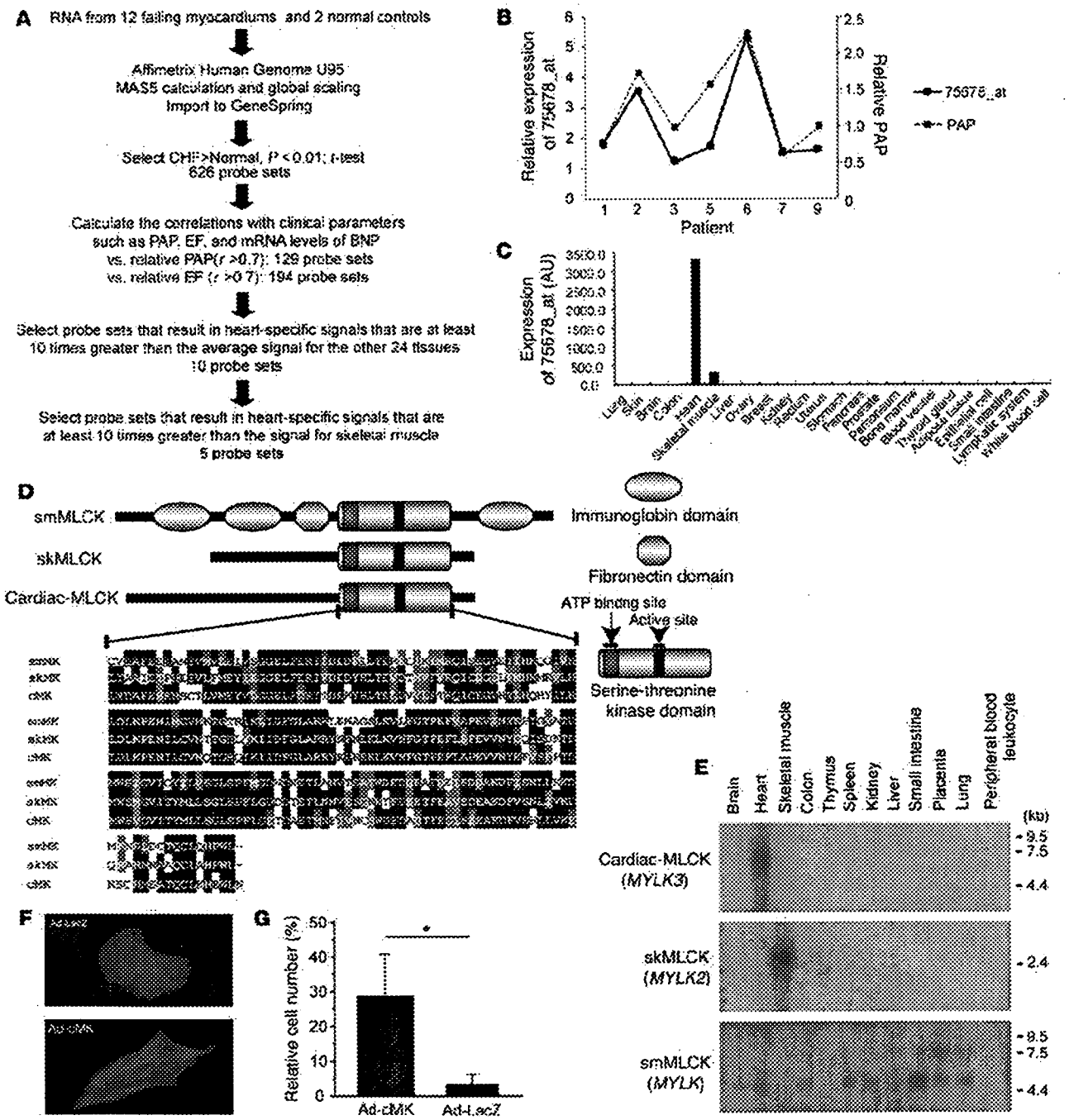

Figure 1

Microarray analysis for candidate gene selection. (**A**) Flowchart for the selection of candidate genes. (**B**) The relative expression levels of 75678_at correlated well with the relative PAP values in the respective patients. (**C**) Tissue localization of the candidate gene expression was analyzed using the GeneExpress database; 75678_at was specifically expressed in the heart. (**D**) Each MLCK family member possesses a highly conserved serine-threonine kinase domain in the C-terminal region of the protein. Amino acid residues on black backgrounds are the most commonly conserved residues at each position; residues on gray backgrounds are similar to the consensus amino acids. (**E**) Expression analysis of MLCK family members using multiple human tissue Northern blot membranes. The 2 transcripts transcribed from *MYLK* (encoding smMLCK) were ubiquitously expressed with the exception of skeletal muscle, thymus, and peripheral blood leukocytes. In contrast, *MYLK2* (encoding skMLCK) and *MYLK3* (encoding cardiac-MLCK) were only expressed in skeletal muscle and heart, respectively. (**F**) Fluorescence microscopy of cardiomyocytes cultured in serum-free conditions and infected with adenovirus encoding LacZ (Ad-LacZ) revealed predominantly round-shaped cells with disorganized sarcomere structures. Infection with adenovirus encoding cardiac-MLCK (Ad-cMK) at a MOI of 120 increased the number of the cells with organized sarcomere structures. Original magnification, ×1,000. (**G**) The percentage of cells with organized sarcomeres was significantly higher in cardiomyocytes infected with adenovirus encoding cardiac-MLCK than in those infected with adenovirus encoding LacZ. Values are mean ± SEM. $^*P < 0.001$.

Next, we generated polyclonal antibodies specific for rodent cardiac-MLCK (RcMK). Antibodies that detected phosphorylated MLC2v (p-s15MLC; anti-rodent serine 15 phosphorylated MLC2v) and total MLC2v (tMLC) were also generated. RcMK detected rat cardiac-MLCK from whole-cell cardiomyocyte extracts as well as recombinant FLAG-tagged murine cardiac-MLCK (Figure 2E). Phosphorylated MLC2v and nonphosphorylated MLC2v could be clearly separated using urea-glycerol gel electrophoresis (12). tMLC detected both phosphorylated and nonphosphorylated MLC2v, whereas p-s15MLC specifically detected the phosphorylated form of MLC2v (Figure 2F). Overexpression of cardiac-MLCK increased the levels of phosphorylated MLC2v in cultured cardiomyocytes (Figure 2G). However, there was no effect on the expression of other sarcomere proteins involved in sarcomere organization such as troponin T, desmin, and α-actinin. mRNA expression of ANP and β myosin heavy chain, representative markers of cardiac hypertrophy, were also unaffected by cardiac-MLCK overexpression (data not shown). To further investigate the phosphorylation of MLC2v by endogenous cardiac-MLCK, we used specific siRNAs targeting cardiac-MLCK (si-cMKs). These siRNAs effectively suppressed the level of cardiac-MLCK mRNA by more than 70%, as determined using quantitative real-time PCR 24 hours after transfection (Figure 2H). These siRNAs also effectively suppressed the level of cardiac-MLCK protein and the amount of phosphorylated MLC2v 60–72 hours after transfection (Figure 2I), whereas no remarkable effects were seen for the expression of other sarcomere proteins. On the contrary, suppression of smMLCK expression, which is also distributed in heart, using siRNA targeting rat smMLCK (si-smMK) did not change either the phosphorylation status of MLC2v or the expression of sarcomere proteins (Figure 2J). These results indicated that cardiac-MLCK predominantly phosphorylates MLC2v, which is selectively expressed in cardiomyocytes. Thus, cardiac-MLCK may regulate morphologic change in cardiomyocytes, including sarcomere organization, through MLC2v phosphorylation.

Cardiac-MLCK regulates sarcomere assembly in cultured cardiomyocytes. To elucidate the precise role of cardiac-MLCK in the sarcomere structure, we analyzed the effects of MLC2v phosphorylation on sarcomeres in cultured neonatal rat cardiomyocytes. Polymerized actin stained with rhodamine-phalloidin revealed a regularly organized pattern of striations (Figure 3A). Phosphorylated MLC2v labeling with p-s15MLC demonstrated a similar striated pattern, although the labeling was predominantly observed in the A-band region, a portion of the sarcomere primarily made up of thick filaments (Figure 3, B–D). Diffuse cytosolic fluorescent labeling was seen when cardiac-MLCK was labeled with RcMK (Figure 3, E–G).

When cardiomyocytes were cultured in serum-free conditions, the organized striation pattern of actin was disrupted and the phosphorylated MLC2v-specific signal decreased (Figure 3K). To evaluate the morphologic changes observed in cardiomyocytes upon activation of endogenous cardiac-MLCK, we treated cardiomyocytes cultured under serum-free conditions with epinephrine. Stimulation of G protein–coupled receptors with epinephrine should activate cardiac-MLCK by increasing intracellular Ca^{2+} concentrations (13). A marked upregulation of MLC2v phosphorylation was obtained following treatment with 2 μM epinephrine (Figure 3H). Epinephrine-induced phosphorylation of MLC2v, which was observed as early as 5 minutes after stimulation, peaked within 30 minutes (Figure 3I). Treatment of the cardiomyocytes cultured in serum-free conditions with 2 μM epinephrine also induced reassembly of sarcomere structures and MLC2v phosphorylation (Figure 3, J, K, and L). To confirm the relevance of MLC2v phosphorylation by cardiac-MLCK, we introduced si-cMKs into cardiomyocytes and analyzed the sarcomere patterns in these cells. The level of phosphorylated MLC2v was reduced 72 hours after transfection with the si-cMKs; however, we did not observe any remarkable changes in the structures of the sarcomeres in cardiomyocytes cultured with serum. The sarcomeres of control siRNA– and si-cMK–treated cells contained organized filament structures (cells with organized sarcomeres, 97.0% ± 1.0% versus 90.0% ± 1.0%; NS; Figure 4, A–F and I). In contrast, the knockdown of cardiac-MLCK produced significant effects on sarcomere reassembly. si-cMK inhibited sarcomere reassembly after epinephrine treatment in cardiomyocytes cultured under serum-free conditions (cells with organized sarcomeres, 76.0% ± 8.5% versus 43.6% ± 7.0%; $P < 0.005$; Figure 4, A–F and I). We also confirmed the phosphorylation of MLC2v using immunoblot analysis (Figure 4G). The results of the immunoblot analysis are quantified in Figure 4H, and the relative MLC2v phosphorylation levels in this experiment exhibited a similar pattern as the percentages of cardiomyocytes with organized sarcomeres (Figure 4I), except in baseline, serum-containing conditions. These data suggest that MLC2v phosphorylation by cardiac-MLCK plays a critical role in initiating sarcomere reassembly.

Cardiac-MLCK is essential for normal cardiac development and function in zebrafish embryos. In order to further evaluate the physiologic roles of cardiac-MLCK, genetically engineered animals must be examined. In mice, however, targeted deletion of the cardiac ventricular myosin light chain, a specific substrate of cardiac-MLCK, was embryonic lethal at embryonic day 12.5 (6). Because cardiac-MLCK is an upstream modulator of MLC2v, deletion of the gene encoding cardiac-MLCK could also be embryonic lethal. Therefore, we performed in vivo knockdown experiments in *Danio rerio*, in which the phenotype generated by disrupting the functions of a targeted gene can be analyzed even if loss of the gene's functions is fatal. First, we generated a zebrafish cDNA library from which we cloned the zebrafish ortholog of *MYLK3* (*zmylk3*; encoding z-cardiac-MLCK). The amino acid sequence of cardiac-MLCK is highly similar to those of other vertebrate orthologs, especially within the C-terminal serine/threonine kinase domain (Figure 5A). Furthermore, like *MYLK3*, *zmylk3* is located between the genes VPS35 and NP001001436.1 (Assembly Zv5sc; Wellcome Trust Sanger Institute), indicating that this was the region of synteny between human and zebrafish. We also performed whole-mount in situ hybridizations using *zmylk3*-specific probes; the results indicated that *zmylk3* was expressed only in the heart at 24 and 48 hours postfertilization (hpf; Figure 5, B–I).

We injected zebrafish embryos with a specific MO directed against the AUG translational start site of the z-cardiac-MLCK mRNA (z-cMKaugMO). At 33 hpf, compared to control mock-injected zebrafish embryos, the heart region was slightly swollen in the z-cMKaugMO morphants. At 48 hpf, ventral swelling was observed in 45.6% ± 6.8% of the z-cMKaugMO morphants (Figure 6A). The ventral swelling became more apparent at 72 hpf (Figure 6B). In contrast, zebrafish embryos injected with an MO containing 5-base mismatches compared with z-cMKaugMO were indistinguishable from control zebrafish embryos (Figure 6C). We further examined the effects of 3 additional MOs, which were targeted to delete specific exons of z-cardiac-MLCK and z-MLC2v. Of these MOs, 2 were directed against the splice donor and acceptor

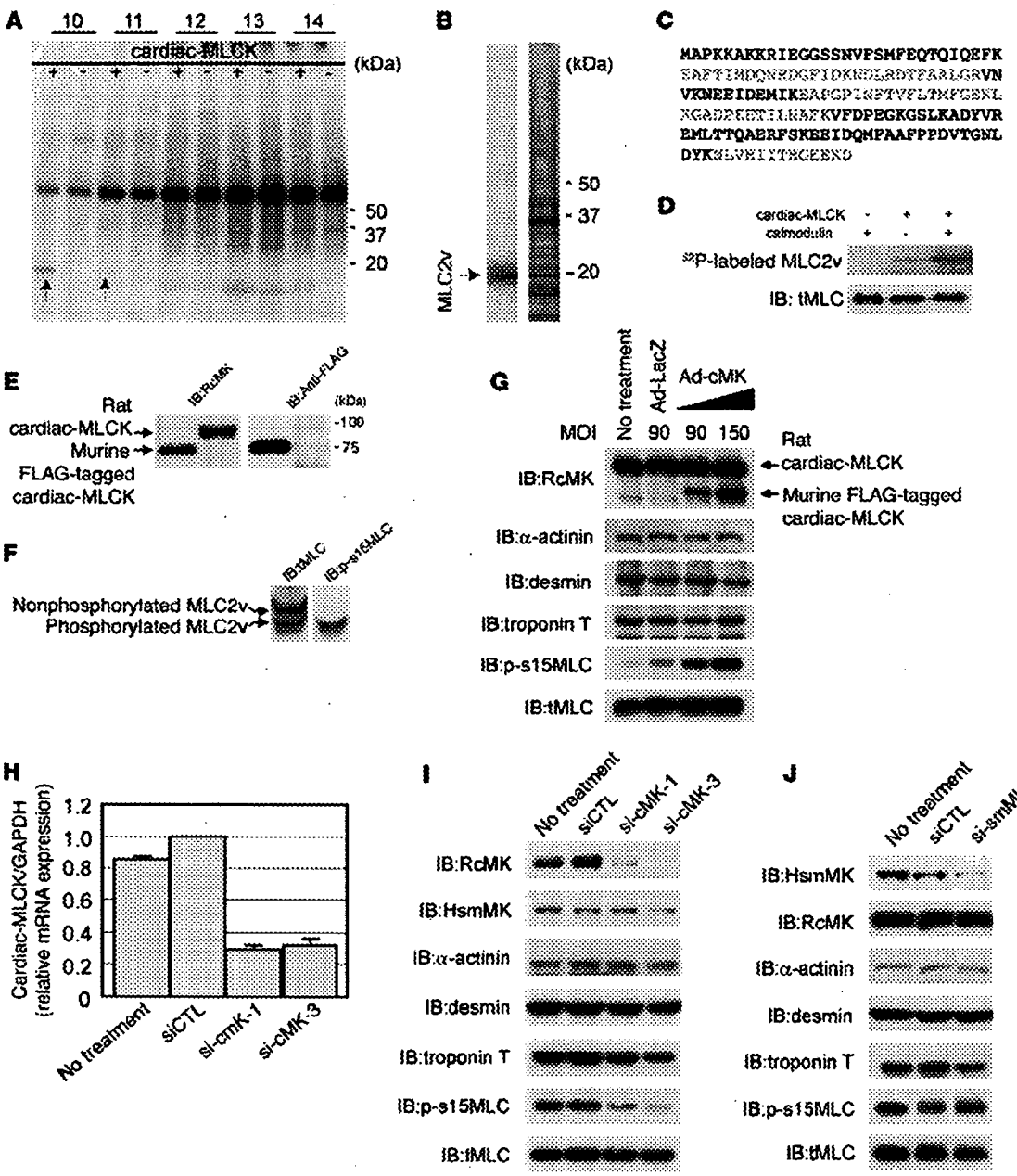

Figure 2

Identification of MLC2v as a specific substrate of cardiac-MLCK. (**A**) A putative 20-kDa substrate that was labeled with P^{32} in the presence of cardiac-MLCK was identified in fractionated murine myocardium extracts (arrows). Fraction numbers are shown at top. (**B**) P^{32}-labeled MLC2v was purified and visualized by autoradiography (left lane) and silver staining (right lane). (**C**) Peptides from the purified protein, which matched the sequences of murine MLC2v, are shown in red. (**D**) Purified MLC2v from murine myocardia was phosphorylated by cardiac-MLCK in a Ca^{2+}-calmodulin–dependent manner. (**E**) RcMK detected rat cardiac-MLCK from cultured cardiomyocyte cell extracts and FLAG-tagged murine cardiac-MLCK. (**F**) Nonphosphorylated MLC2v and phosphorylated MLC2v were separated using urea-glycerol gel electrophoresis. tMLC and p-s15MLC were confirmed to specifically detect each target protein. (**G**) Overexpression of murine cardiac-MLCK in cultured cardiomyocytes following infection with an adenovirus vector encoding murine cardiac-MLCK at MOIs of 90 and 150 upregulated the phosphorylation of MLC2v in a dose-dependent manner. Endogenous rat cardiac-MLCK is shown at top; overexpressed murine cardiac-MLCK is shown below. (**H** and **I**) Both si-cMK-1 and si-cMK-3 effectively suppressed the mRNA (**H**) and protein levels (**I**) of cardiac-MLCK, resulting in reduced phosphorylation of MLC2v. smMLCK, α-actinin, desmin, and troponin T were not affected by suppression of cardiac-MLCK expression. siCTL, control siRNA. (**J**) The protein levels of smMLCK were effectively decreased by si-smMK; no remarkable changes were observed in protein levels of phosphorylated MLC2v or other sarcomere-related proteins.

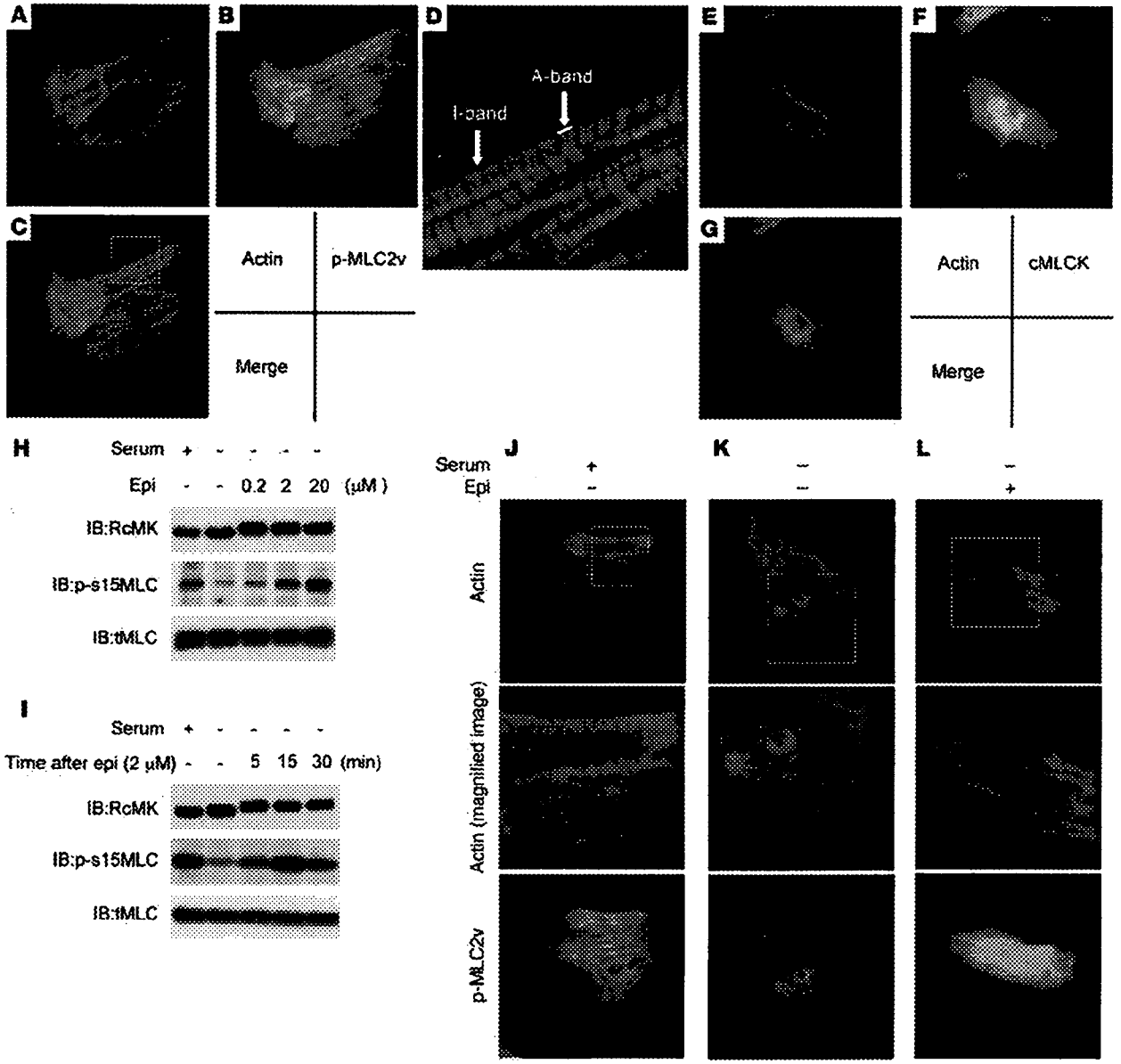

Figure 3

Epinephrine treatment induced sarcomere assembly through MLC2v phosphorylation. Original magnification, ×1,000 (**A–C** and **E–G**). (**A–D**) Polymerized actin stained with rhodamine-phalloidin (**A**) as well as phosphorylated MLC2v labeled with p-s15MLC (**B**) exhibited regular patterns of striation. (**C**) Merged image of **A** and **B**. (**D**) Higher magnification of boxed area in **C** revealed that rhodamine-phalloidin predominantly stained the I-band, whereas phosphorylated MLC2v (p-MLC2v) was localized in the A-band. Original magnification, ×4,000 (**D**). (**E–G**) Cardiac-MLCK (cMLCK) labeled with RcMK showed a diffuse cytosolic labeling pattern. (**H**) Cultured cardiomyocytes were stimulated with 0.2–20 μM epinephrine (Epi), which upregulated MLC2v phosphorylation in a dose-dependent manner. (**I**) Cultured cardiomyocytes were stimulated with 2 μM epinephrine for the indicated time periods. Epinephrine-induced phosphorylation of MLC2v in cultured cardiomyocytes was observed as early as 5 minutes after stimulation; maximal phosphorylation was obtained after approximately 30 minutes. (**J–L**) Cardiomyocytes cultured with serum contained organized patterns of striation and a moderate level of MLC2v phosphorylation. Middle panels show higher magnification of boxed regions in top panels. Cardiomyocytes cultured in serum-free conditions were incubated in the absence (**K**) or presence (**L**) of 2 μM epinephrine. (**K**) Cardiomyocytes cultured under serum-free conditions contained disorganized, punctuated actin staining with a reduced level of MLC2v phosphorylation. (**L**) Stimulation with epinephrine provoked rapid sarcomere reassembly and augmented MLC2v phosphorylation. Original magnification, ×1,000 (**J–L**, upper and lower panels); ×3,000 (**J–L**, middle panels).

sites of exons 4 and 6 of z-cardiac-MLCK, respectively. Deletion of exon 4 caused a frameshift and resulted in premature termination of the transcript. Exon 6 includes the catalytic center of z-cardiac-MLCK, and its deletion was expected to diminish the protein's kinase activity. The third MO was designed to delete exon 2 of z-MLC2v, which includes the phosphorylatable serine. These 3

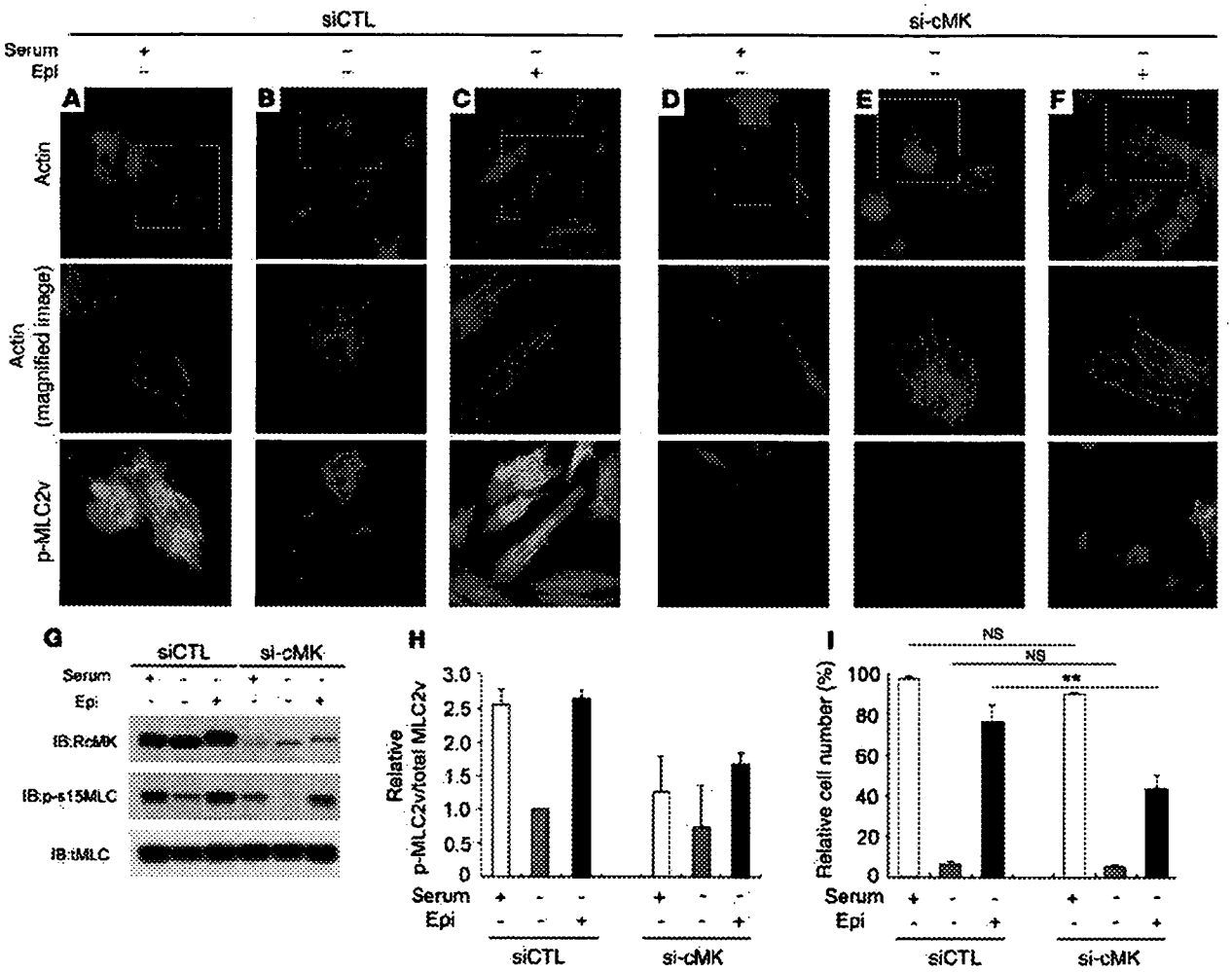

Figure 4

Cardiac-MLCK regulates the initiation of sarcomere assembly in cultured cardiomyocytes through MLC2v phosphorylation. Original magnification, ×1,000 (upper and lower panels); ×2,000 (middle panels). (**A–F**) Cardiomyocytes were transfected with control siRNA (**A–C**) or si-cMK (**D–F**). Middle panels show higher magnification of boxed regions in top panels. In serum-containing conditions, si-cMK–transfected cardiomyocytes showed reduced levels of MLC2v phosphorylation (**D**) compared with control siRNA–transfected cardiomyocytes (**A**), although both exhibited regularly organized sarcomere structures. Actin staining in cardiomyocytes cultured in serum-free conditions revealed a punctuated pattern in the sarcomeres (**B** and **E**); moreover, the degree of MLC2v phosphorylation was reduced in the si-cMK–transfected cardiomyocytes compared with the control siRNA–transfected cardiomyocytes. Stimulation with 2 μM epinephrine provoked upregulation of MLC2v phosphorylation and sarcomere reassembly in control siRNA–transfected cardiomyocytes (**C**), but not in si-cMK–transfected cardiomyocytes (**F**). (**G**) We confirmed the levels of MLC2v phosphorylation shown in **A–F** using immunoblot analysis. (**H**) Quantitation of the levels of phosphorylated MLC2v shown in **G**. Values are mean ± SEM. (**I**) Percentage of the cells with organized sarcomeres. There was no significant difference between the populations of cardiomyocytes transfected with control siRNA and si-cMK under either serum-containing or serum-free conditions. The percentage of the cells with organized sarcomeres was significantly higher for the control siRNA–transfected cardiomyocytes than for the si-cMK–transfected cardiomyocytes. Values are mean ± SEM. p-MLC2v, phosphorylated MLC2v. $^{**}P < 0.001$.

MOs effectively deleted the targeted exons, inducing comparable ventral swelling phenotypes (Figure 6, D–F). The finding that 4 different MOs produced similar results suggests that the cardiac phenotypes resulted from a loss of the kinase activity of z-cardiac-MLCK. To evaluate the cardiac phenotype of the z-cMKaugMO morphants in detail, we examined the SAG4A zebrafish strain, which specifically expresses GFP in the cardiac ventricle (14). After injecting z-cMKaugMO into SAG4A embryos, cardiac motion at 72 hpf was imaged with a high-sensitivity digital camera attached to a fluorescence stereomicroscope (Figure 6G and Supplemental Movies 1 and 2; supplemental material available online with this article; doi:10.1172/JCI30804DS1). Recordings were converted to motion mode (M-mode) images using our original software (Figure 6H). From these images, we determined the end-diastolic dimension (Dd), end-systolic dimension (Ds), and fractional shortening (FS) of the cardiac ventricle. These data are summarized in Table 2, and the results indicate that the cardiac dimensions of the z-cMKaugMO morphants were significantly larger than those of control zebrafish embryos (Dd, 79.6 ± 3.7 versus 117.0 ± 10.4 μm; Ds, 50.3 ± 6.5 versus 76.0 ± 7.0 μm; $P < 0.0001$ for both com-

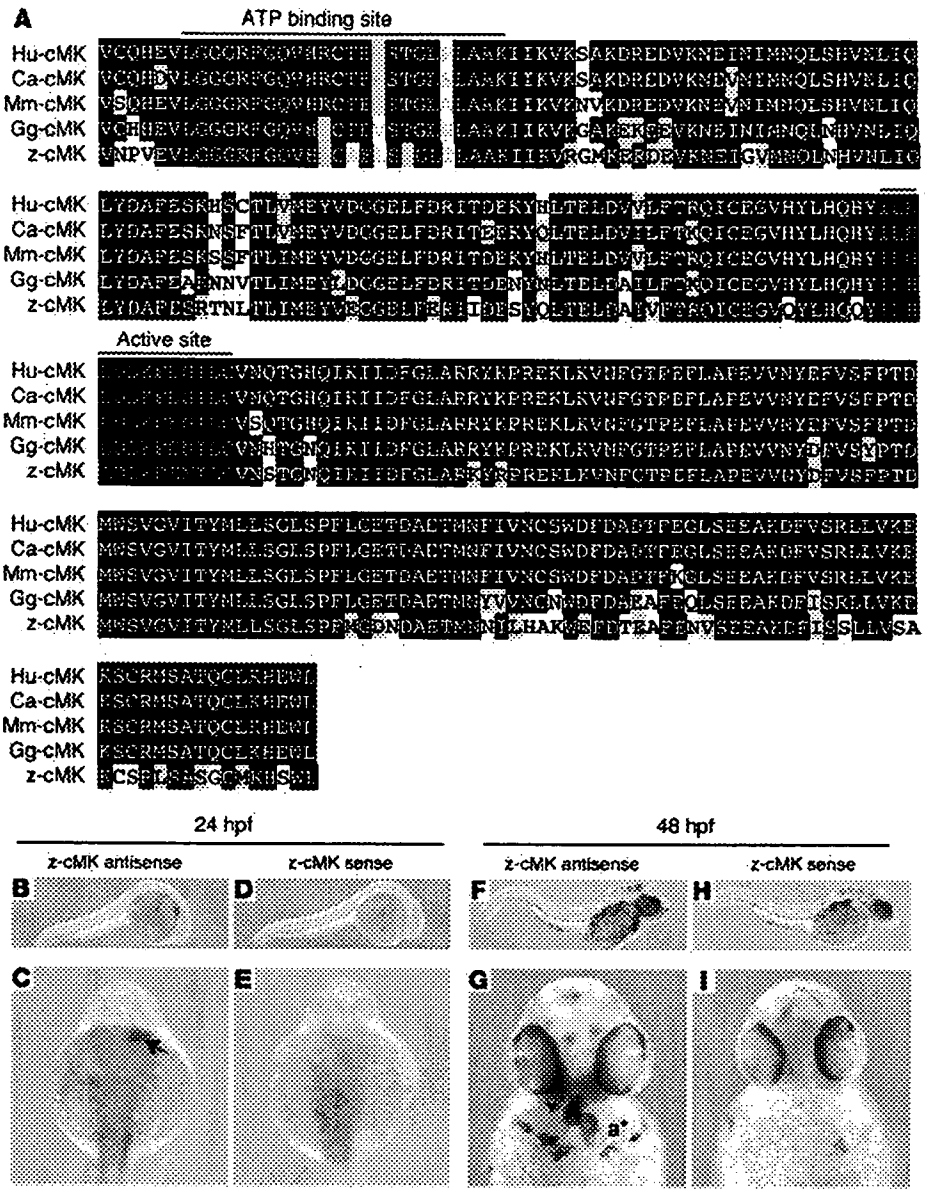

Figure 5
Cardiac-MLCK is highly conserved in several vertebrates, including zebrafish. (**A**) Cardiac-MLCK is evolutionarily conserved in vertebrates, including humans (Hu), dogs (Ca), mice (Mm), chickens (Gg), and zebrafish (z), with the highest degree of homology in the C-terminal portion of the serine/threonine kinase domain. Black backgrounds indicate identical amino acids. Amino acids in the ATP-binding region are shown in blue; those in the kinase active site are shown in red. (**B–I**) Whole-mount in situ hybridizations depict the expression of z–cardiac-MLCK (z-cMK) in zebrafish embryos hybridized with z–cardiac-MLCK–specific antisense probe (**B**, **C**, **F**, and **G**) or z–cardiac-MLCK sense probe (**D**, **E**, **H**, and **I**). At 24 hpf, z–cardiac-MLCK was expressed in heart precursor cells (arrow). At 48 hpf, z–cardiac-MLCK was selectively expressed in the heart (asterisks denote atrium [a] and ventricle [v]).

parisons). We did not, however, observe a significant difference in cardiac contractility as assessed by the FS (36.9% ± 7.1% versus 34.9% ± 4.1%; NS), likely because of a compensatory upregulation of inotropy. In support of this hypothesis, we observed that the heart rate was significantly higher in the z-cMKaugMO morphants (184 ± 14.5 versus 216 ± 24.7 bpm; $P = 0.0017$). At 5–6 days after fertilization, the z-cMKaugMO morphants developed systemic edema and died of circulatory disturbances. Histopathologic analysis demonstrated that the ventral swelling in the z-cMKaugMO morphants reflected pericardial edema. Although the cardiac atria were almost normal, the ventricular walls of the morphants were thinner than those of control zebrafish embryos (Figure 7, A–D). Transmission electron microscopy revealed that only a few poorly differentiated sarcomere structures were present in the ventricles of the z-cMKaugMO morphants (Figure 7, G–J); no other apparent abnormalities were detected in the atrial sarcomeres (Figure 7, E and F). These data suggest that cardiac-MLCK is required for sarcomere formation in the developing heart.

Cardiac-MLCK is upregulated during myofibrillogenesis and in mammalian models of heart failure. Sarcomere organization in cardiomyocytes in vivo is supposed to occur during myofibrillogenesis. In the rat heart, the mRNA and protein levels of cardiac-MLCK were upregulated from 1 week after birth through adulthood (Figure 8, A and B). The expression of cardiac-MLCK mRNA was also analyzed in mammalian models of heart failure. Myocardial infarctions (MIs) were produced in Wistar rats by permanently ligating the left anterior descending artery. At 4 weeks after the onset of MI, heart failure developed. The hemodynamic and echocardiographic parameters of the MI and sham-operated rats are summarized in Table 3. In MI rats, the LV end-diastolic pressure and LVDd were significantly higher than in sham-operated rats (LV end-diastolic pressure, 20.5 ± 8.2 versus 3.2 ± 1.0 mmHg; $P < 0.01$;

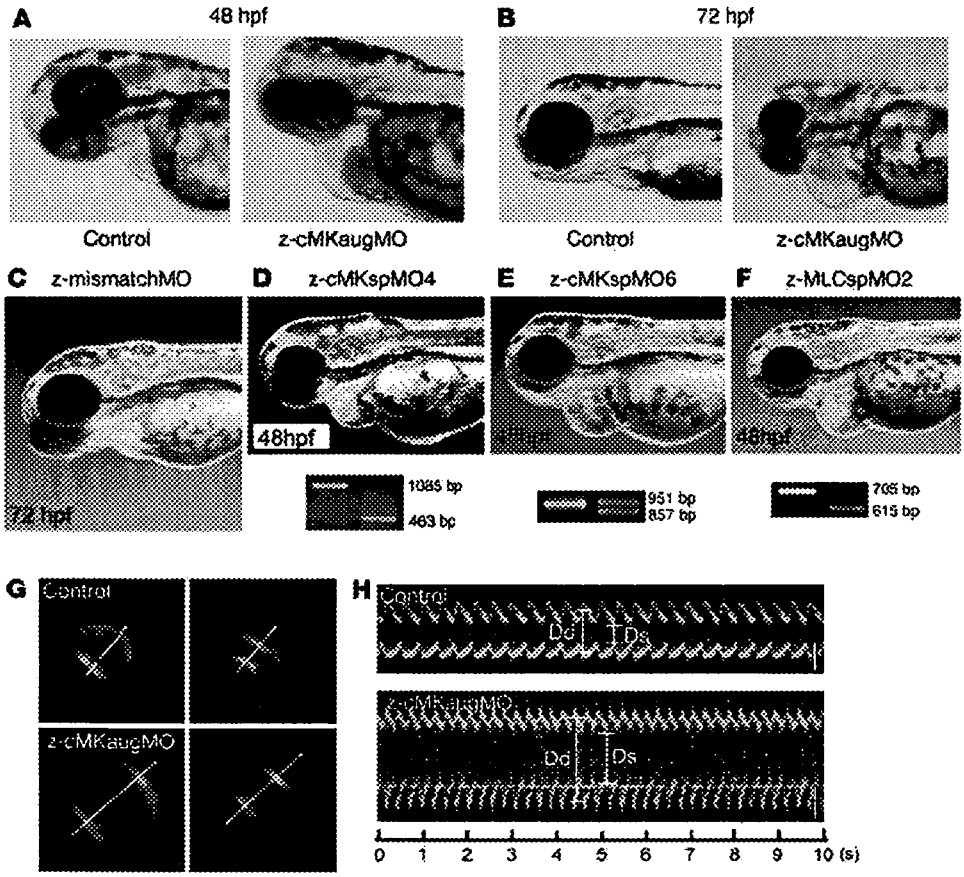

Figure 6

Suppression of z–cardiac-MLCK expression induced dilatation of the cardiac ventricle in zebrafish embryos. (**A** and **B**) Control mock-injected zebrafish embryos and zebrafish embryos injected with z-cMKaugMO produced the phenotype of ventral swelling at 48 hpf (**A**) and 72 hpf (**B**). (**C**) Zebrafish embryos injected with MOs with 5-base mismatch to z-cMKaugMO (z-mismatchMO) showed phenotypes comparable to those of controls. (**D** and **E**) Injection of specific MOs designed to interfere with the splicing of z–cardiac-MLCK exon 4 (z-cMKspMO4; **D**) or exon 6 (z-cMKspMO6; **E**) or with the splicing of z-MLC2v exon 2 (z-MLCspMO2; **F**), which coded for the phosphorylatable serine residue, also induced the phenotype of ventral swelling. RT-PCR products amplified from cDNA produced from the morphants were shorter than those obtained from control embryos due to the removal of the targeted exons. (**G**) Cardiac motion in the control embryos and z-cMKaugMO morphants. Shown are end-diastolic (left) and end-systolic (right) phases of the cardiac ventricular cycle in a control embryo and z-cMKaugMO morphant. (**H**) Representative M-mode images of both control embryo and z-cMKaugMO morphant hearts. Scale bars: 50 μm. Original magnification, ×20 (**A**–**F**); ×100 (**G**).

LVDd, 9.8 ± 0.3 versus 6.8 ± 0.5 mm; $P < 0.01$), whereas the maximum LV peak rate of change in pressure during isovolumic contraction (Max dP/dt) and FS were significantly lower than in sham-operated rats (Max dP/dt, 5,845 ± 1,156 versus 9,440 ± 644 mmHg/s; $P < 0.01$; FS, 12.0 ± 3.1 versus 44.0 ± 7.8%; $P < 0.01$). In MI rats, *MYLK3* expression was significantly upregulated compared with that in the sham-operated rats (relative cardiac-MLCK mRNA expression, 1.46 ± 0.42 versus 1.00 ± 0.15; $P < 0.05$; Figure 8C). Furthermore, the relative mRNA expression level of cardiac-MLCK was significantly correlated with that of ANP ($r = 0.778$, $P < 0.005$; Figure 8D). Upregulation of cardiac-MLCK expression in the infantile heart suggests cardiac-MLCK participates in myofibrillogenesis. Additionally, upregulation of cardiac-MLCK mRNA levels in mammalian models of heart failure confirmed the results obtained with the microarray analysis of human failing myocardia.

Discussion

In this study, we performed microarray analysis of human failing myocardia to identify new genes involved in the pathophysiology of CHF. By comparing mRNA expression analysis with the clinical parameters of the patients, we identified what we believe to be a novel candidate gene, *MYLK3* (encoding cardiac-MLCK), that had not been isolated in previous microarray studies of heart failure (15). Upregulation of *MYLK3* transcription in failing myocardia was confirmed in mammalian models of heart failure, such as MI rats. In this experiment, mRNA expression of cardiac-MLCK was significantly upregulated in MI rats with heart failure, and the relative expression profile was well correlated with that of ANP, a representative marker of CHF.

MLCK family members in muscle are sarcomeric protein kinases that phosphorylate a serine residue near the amino terminus of the myosin regulatory light chain. In cardiac muscle, phosphorylation of MLC2v led to sarcomere organization, an event that represents cardiac hypertrophy in cultured neonatal rat cardiomyocytes (13). skMLCK is thought to be the predominant kinase that acts on MLC2v, and a gradient of MLC2v phosphorylation in the cardiac wall from endocardium to epicardium is responsible for the generation of cardiac torsion (9). A recent study using skMLCK-deficient mice, however, revealed that removing skMLCK did not result in a cardiac phenotype (10). Furthermore, in the current study and previous studies, skMLCK expression was not detected in the heart by either Western blotting or RT-PCR (16), suggesting the existence of an as-yet unknown kinase that phosphorylates MLC2v in cardiac muscle.

We identified cardiac-MLCK, which serves as a specific kinase for MLC2v in cardiac muscle. In cultured cardiomyocytes, cardiac-MLCK regulates sarcomere assembly through the phosphorylation of MLC2v. When isolated cardiomyocytes were cultured under serum-free conditions, established sarcomere structures were disrupted. Overexpression of recombinant cardiac-MLCK and exogenous stimulation by epinephrine promoted sarcomere

Table 2
Cardiac physiological characteristics of control and morphant zebrafish embryos

	Control	Morphant	*P*
Dd (μm)	79.6 ± 3.7	117 ± 10.4	<0.0001
Ds (μm)	50.3 ± 6.5	76.0 ± 7.0	<0.0001
FS (%)	36.9 ± 7.1	34.9 ± 4.1	NS
HR (bpm)	184 ± 14.5	216 ± 24.7	0.0017

Values are mean ± SEM. n = 12 per group. HR, heart rate.

reassembly through MLC2v phosphorylation. Similar findings have previously been reported using recombinant constitutively active skMLCK (13). We further elucidated the physiologic roles of endogenous cardiac-MLCK using siRNAs. Decreases in MLC2v phosphorylation following the introduction of si-cMK significantly impaired epinephrine-induced sarcomere reassembly. Additionally, specific knockdown of cardiac-MLCK did not affect to the expression of other sarcomere-related proteins such as troponin T, desmin, and α-actinin. These proteins are thought to have important roles in sarcomere and myofibril formation (17–19). Thus, in cardiomyocytes, phosphorylation of MLC2v by cardiac-MLCK is an essential step for the initiation of sarcomere assembly. Upregulation of the protein levels of cardiac-MLCK in infantile rat heart supports this idea.

In this experimental model, no phenotypic alterations were observed following knockdown of cardiac-MLCK in cultured cardiomyocytes. This apparently paradoxical result occurred because phosphorylation of MLC2v is upregulated in cultured cardiomyocytes until 36 hours after plating, after which it is gradually downregulated. In the siRNA-mediated gene knockdown experiment, a reduction in the cardiac-MLCK protein level that was sufficient to decrease the phosphorylation of MLC2v was only obtained 60–72 hours after isolation. Therefore, by the time the required level of protein suppression was achieved, primary sarcomere assembly had been completed, and the subsequent decreases in MLC2v phosphorylation did not disrupt established sarcomere structures.

Reduction of cardiac-MLCK levels in zebrafish embryos through the injection of z-cMKaugMO resulted in ventral swelling, which has been previously reported to be a representative phenotype of cardiac abnormalities in zebrafish embryos (20, 21). The reliability of the results obtained with z-cMKaugMO was confirmed using multiple MOs that targeted not only cardiac-MLCK but also its substrate, MLC2v. In each experiment, reproducible results were obtained. Another MO that has 5-base mismatch to z-cMKaugMO was also examined as a negative control MO. Further analysis revealed dilatation of the ventricle with a thinned ventricular wall and immature sarcomeres in the morphants. The fragility of the ventricular wall as a result of insufficient sarcomere formation may have caused the ventricular dilatation. Although ventricular function as assessed by FS was preserved in the morphants, this might have been due to some positive inotropic effects, which were suggested by the increased heart rate observed in the z-cMKaugMO morphants. Although several reports have investigated the effects of MLC2v phosphorylation in striated muscle contractions, including in cardiac muscle, the in vivo ventricular role of MLC2v phosphory-

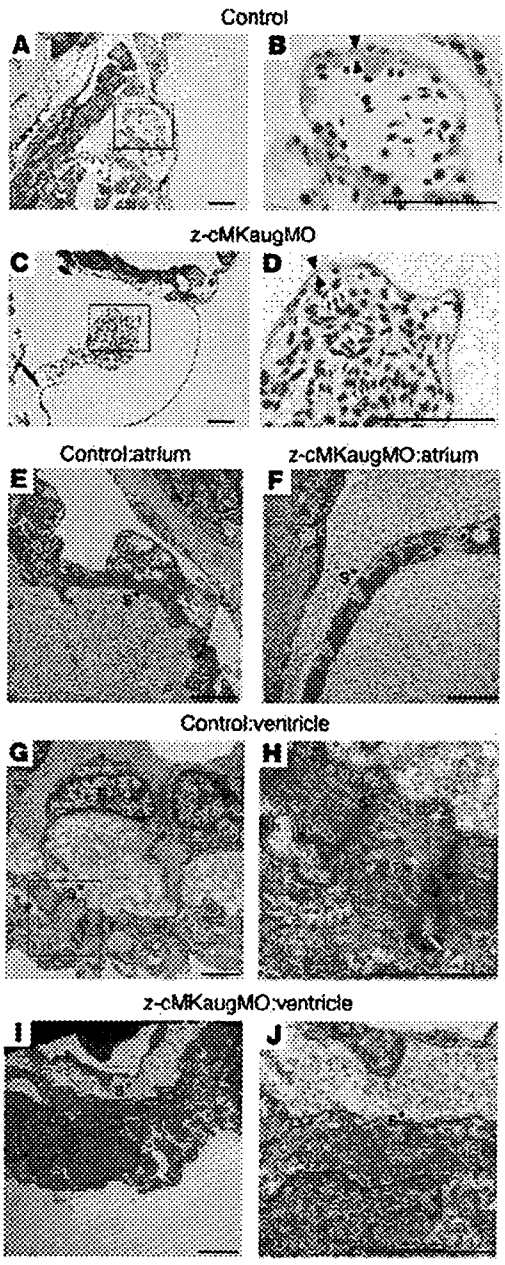

Figure 7
Histology of the zebrafish heart at 48 hpf. (**A–D**) Longitudinal sections stained with hematoxylin and eosin. Scale bars: 50 μm. (**E–J**) Transmission electron micrographs. Scale bars: 2 μm. (**A** and **B**) Histology of control zebrafish hearts at 48 hpf. A relatively thick ventricular wall was apparent (**B**, arrowheads). (**C** and **D**) Pericardial edema and a thinner ventricular wall (**D**, arrowheads) were observed in z-cMKaugMO morphants. (**E** and **F**) In the atria, the sarcomere structures were well differentiated in both the control embryos and the z-cMKaugMO morphants. In the ventricles of control embryos, robust sarcomere structures were observed (**G** and **H**), whereas the ventricles of the z-cMKaugMO morphants contained sparse and immature sarcomere structures (**I** and **J**). Images in **B**, **D**, **H**, and **J** show higher magnifications of the boxed areas in **A**, **C**, **G**, and **I**, respectively. Asterisks denote sarcomere structures (s).

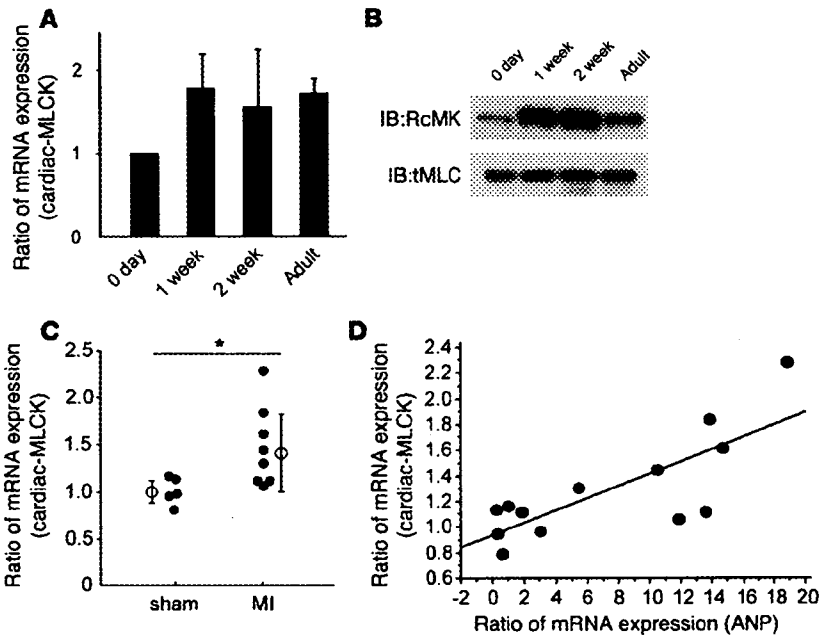

Figure 8
Expression of cardiac-MLCK is upregulated in infantile rat myocardia and failing rat myocardia. (**A**) mRNA expression of cardiac-MLCK was also upregulated in rat myocardia from 1 week after birth to adulthood. The levels of cardiac-MLCK protein were upregulated in infantile myocardia 1–2 weeks after birth. (**B**) The levels of cardiac-MLCK protein were upregulated in infantile myocardia 1–2 weeks after birth. (**C**) mRNA expression of cardiac-MLCK was significantly upregulated in failing rat myocardia. $n = 5$ (sham-operated); 8 (MI). Filled symbols represent values from individual mice; open symbols with bars represent mean ± SEM. $^*P < 0.05$. (**D**) The relative mRNA expression levels of ANP and cardiac-MLCK were significantly correlated ($r = 0.778$; $P < 0.005$).

lation is still not well understood (22, 23). To explore how cardiac-MLCK contributes to ventricular function, other experiments, such as a skinned fiber study, should be performed. A similar cardiac phenotype was reported in a recent study investigating the zebrafish *tel* mutant, in which the gene encoding MLC2v was disrupted by an *N*-ethyl-*N*-nitrosourea-induced mutation. The authors concluded that MLC2v is essential for the assembly of myosin thick filament (24). The observation of incomplete sarcomere formation resulting in a dilated ventricle in zebrafish embryos after injection of z-cMKaugMO can be explained by an inability to initiate sarcomere assembly as a result of reduced cardiac-MLCK levels.

Our results prompt the important question of how cardiac-MLCK is involved in the pathophysiology of CHF. In failing myocardia, decreases in myofibrillar proteins such as titin, myosin, and actin, together with the sarcomere defects, have been identified (25, 26). Reduced expression of MLC2v protein as a result of protease-mediated cleavage and reduced phosphorylation of MLC2v have also been reported in the myocardia of patients with dilated cardiomyopathy. These changes produced unstable, short myofilaments following defective assembly of the myosin thick filaments (27, 28). Our preliminary data also revealed that the protein expression of cardiac-MLCK and the extent of MLC2v phosphorylation were remarkably decreased in failing myocardia of trans-aortic constriction mice compared with those of sham-operated mice. Previous reports and our present results suggest that cardiac-MLCK may be upregulated to compensate for the lower expression and reduced phosphorylation of MLC2v. As a possible therapeutic modality in patients with CHF, upregulation of cardiac-MLCK may promote sarcomere reassembly and enhanced contractility of the failing heart.

Methods

Animals. All procedures were performed in conformity with the *Guide for the care and use of laboratory animals* (NIH publication no. 85-23, revised 1996) and were approved by the Osaka University Committee for Laboratory Animal Use.

Materials. We used commercially available anti-FLAG-M2 antibody and anti-FLAG-M2 affinity gel (Sigma-Aldrich), monoclonal mouse anti-troponin T cardiac isoform antibody (NeoMarkers), monoclonal mouse anti-human desmin Antibody (Dako Corp.), and polyclonal goat anti-α-actinin (N-19) antibody (Santa Cruz Biotechnology Inc.). Epinephrine hydrochloride was purchased from Sigma-Aldrich. We also generate RcMK, anti-human smMLCK, tMLC, and p-s15MLC.

Microarray analysis. For microarray analysis, 2 RNA samples of human normal myocardium and 12 samples of failing myocardium were used. Failing myocardium samples were obtained from severe CHF patients by Batista or Dor operation after obtaining the patients' written informed consent. PAP was measured 2–4 weeks before the operation, and ejection fraction (EF) was measured by echocardiography the day before the operation. Normal samples were purchased from Biochain Inc. Cardiac gene expression was determined using the HG-U95 Affymetrix GeneChip. All expression data were normalized by global scaling and analyzed by GeneSpring software (Agilent Technologies). All expression data were normalized per gene and analyzed after removing noise and unreliable data. PAP, EF, and BNP values were normalized to their median values, and the correlation between gene expression and the clinical parameters was evalu-

Table 3
Hemodynamic and echocardiographic characteristics of MI and sham-operated rats

	Sham	MI	*P*
LVSP (mmHg)	126.8 ± 10.9	125.5 ± 11.0	NS
HR (bpm)	415.4 ± 10.4	407.6 ± 23.0	NS
Max dP/dt (mmHg/s)	9,440 ± 644	5,845 ± 1,156	<0.01
LVEDP (mmHg)	3.2 ± 1.0	20.5 ± 8.2	<0.01
LVDd (mm)	6.8 ± 0.5	9.8 ± 0.3	<0.01
FS (%)	44.0 ± 7.8	12.0 ± 3.1	<0.01

Values are mean ± SEM. $n = 5$ (sham); 8 (MI). LVEDP, LV end-diastolic pressure; LVSP, LV systolic pressure; HR, heart rate; Max dP/dt, LV peak rate of change in pressure during isovolumic contraction.

ated. To further select genes that are expressed almost exclusively in heart, expression values for the candidate genes were retrieved in 24 major tissues for analysis from GeneExpress database (Gene Logic Inc.) containing GeneChip expression profiles of human samples.

RNA extraction, RT-PCR, and quantification. Rat tissues (20–50 mg) and zebrafish embryos at 72 hpf were homogenized in 1 ml RNA-Bee reagent (Tel-Test Inc.), and total RNA was isolated and converted to cDNA using Omniscript RT kit (QIAGEN) according to the manufacturer's instructions. Specific primers to amplify rat ANP, β myosin heavy chain, cardiac-MLCK, and GAPDH mRNA were purchased from Applied Biosystems. Quantitative RT-PCR reactions were run in duplicate using the ABI Prism 7700 Sequence Detector System (Applied Biosystems). The level of each transcript was quantified by the threshold cycle (Ct) method using GAPDH as an endogenous control. For RT-PCR, specific primers that cover the region of targeted exons were designed to amplify the transcripts of z-cardiac-MLCK and z-MLC2v. See Supplemental Methods for primer sequences.

Northern blot analysis. Commercially available human multiple tissue Northern blot and polyA$^+$ RNA of human heart and skeletal muscle were purchased from Clontech. Each polyA$^+$ RNA was reverse transcribed and amplified using an Omniscript RT kit (QIAGEN) according to the manufacturer's protocol. Hybridization probes of human cardiac-MLCK and smMLCK were amplified by PCR from cDNA of human heart, and a hybridization probe of human skMLCK was amplified by PCR from cDNA of human skeletal muscle. Membrane was hybridized to ^{32}P-labeled probe in Rapid-Hyb buffer (Amersham Bioscience) at 65°C for 1 hour. Final wash conditions were 0.1× SSC with 0.1% SDS at 65°C for 5 minutes. Hybridized membrane was visualized by autoradiography using the BAS system (Fuji).

Preparation and transfection of adenovirus constructs. Adenovirus constructs were generated using ViraPower Adenoviral Expression System (Invitrogen) essentially as instructed by the manufacturer. Adenovirus vectors encoding murine cardiac-MLCK and LacZ were infected to cultured cardiomyocytes for 12 hours in various MOIs. Protein collection and immunostaining were performed 48 hours after adenovirus infection.

Identification of the substrate of cardiac-MLCK. Recombinant cardiac-MLCK was expressed in HEK293T cells as FLAG-tagged protein. HEK293T cells expressing FLAG-tagged cardiac-MLCK were lysed with cell lysis buffer (20 mM MOPS, pH 7.0, 0.15 M NaCl, 10% glycerol, and 1% CHAPS) and recombinant cardiac-MLCK was purified by immunoprecipitation using anti-FLAG-M2 affinity gel (Sigma-Aldrich). Hearts dissected from male C57BL/6 mice (10–12 weeks of age) were mechanically homogenized using a Polytron homogenizer in 10 ml of tissue lysis buffer (30 mM MOPS, pH 6.8, 5% glycerol, 0.1% 2-mercaptoethanol, and 1 mM EGTA). Lysate was centrifuged for 40 minutes at 100,000 *g*, and 9 ml of supernatant was collected. Murine heart extracts were then applied to SP650 cation exchange column. The column was equilibrated with elution buffer A (30 mM MOPS, 5% glycerol, 0.1% 2-mercaptoethanol) at pH 6.8, and the extracts were eluted with a linear gradient of NaCl (0–0.5 M) at a flow rate of 1 ml/min. Each 1-ml fraction collected was incubated for 30 minutes with activated recombinant cardiac-MLCK, commercially available recombinant calmodulin (Upstate), 2 mM $CaCl_2$, and [γ-P^{32}]ATP and then subjected to SDS-PAGE. After drying, the gel was autoradiographed and visualized with BAS (Fuji). The fractions containing 20-kDa substrate (fractions 10 and 11) labeled with [γ-P^{32}]ATP were pooled and applied to a phenyl-RPLC column (5Ph-AR-300; nacalai tesque) equilibrated with 0.3% trifluoroacetic acid and 5% acetoritrile. Fractions were eluted with a linear gradient of 100% acetonitrile at flow rate of 1 ml/min. After separation with SDS-PAGE, the gel was simultaneously silver stained and autoradiographed. After identifying the 20-kDa substrate with silver-stained gel, the bands were excised from the gel, and proteins were identified by matrix-assisted laser desorption/ionization-time-of-flight mass spectrometry and peptide mass fingerprinting.

Preparation of cultured neonatal rat cardiomyocytes and gene silencing via RNA interference. Primary cultures of neonatal cardiomyocytes were prepared from Wistar rats as described previously (29). Cardiomyocytes were cultured in DMEM (Sigma-Aldrich) supplemented with 10% FBS (Equitech-Bio). At 6 hours after isolation of cardiomyocytes, cells were transfected with siRNAs (100 nmol/l) using Optifect reagent (Invitrogen) according to the manufacturer's instructions. Both si-cMK (see Supplemental Methods) and si-smMK (see Supplemental Methods) were purchased from B-bridge. As a negative control, cells were transfected with siControl Non-Targeting siRNA#1 (B-bridge). Isolation of mRNA was performed at 24 hours after transfection and protein experiments were performed at 72 hours after transfection. For immunostaining, the same procedures of siRNA transfection were performed in one-fifth scale on Lab-Tek Chamber Slides (nunc).

Cloning of z–cardiac-MLCK. We generated an adult zebrafish cDNA library in Lambda Zap II (Stratagene) using polyA$^+$ RNA from adult zebrafish. The cDNA library was screened with the probe designed to the 5′ side in the ORF of the putative zebrafish ortholog of cardiac-MLCK sequence. Positive phage clone was determined by using phage plaque screen method and single clone excision protocol according to the manufacturer's instructions (Stratagene).

Gene accession numbers. DDBJ accession numbers for the zebrafish MLCK family were as follows: cardiac-MLCK, AB267907; smMLCK, AB267908; skMLCK, AB267909.

Whole-mount in situ hybridization. The digoxigenin-labeled antisense and sense RNA probes (see Supplemental Methods) were transcribed using SP6 and T7 RNA polymerase. Zebrafish embryos at 24 and 48 hpf were fixed with 4% paraformaldehyde, digested with proteinase K, and hybridized with each probe at 68°C. Alkaline-conjugated anti-digoxigenin antibody was used to detect the signals. After staining, embryos were refixed with 4% paraformaldehyde and stored in PBS.

Injection of MO. All MOs were synthesized by Gene-Tools. At cell stages 1–4, 4–10 ng of these MOs were injected into zebrafish embryos. Several data were collected before the 96-hpf stage. Sequences of MOs are available in the Supplemental Methods.

Analysis of zebrafish cardiac histology and cardiac function. We studied hearts of control mock-injected zebrafish embryos and z-cMKaugMO–injected zebrafish embryos at 72 hpf by routine histopathology including transmission electron micrography. To visualize the motion of zebrafish cardiac ventricle, the SAG4A strain of zebrafish, which specifically expresses GFP in its cardiac ventricular wall (14), was applied to MO-mediated gene knockdown experiments. GFP-expressed control mock-injected and z-cMKaugMO–injected zebrafish hearts at 72 hpf were imaged with Leica digital camera DFC 350 FX on a Leica MZ 16 FA fluorescence stereomicroscope. Acquired images were compiled as digital movie files using Leica FW4000 software. Each recorded movie was converted to M-mode image using our original software, and Dd, Ds, FS, and heart rate were measured from the M-mode images.

Experimental protocols of rats. Male Wistar rats (0 days, 1 week, 2 weeks, and 10 weeks for mRNA and protein expression analysis; 8 weeks for production of MI rats; Japan Animals) were used in these experiments. MI was induced by permanent ligation of the left anterior descending coronary artery as previously described (29). The same surgical procedure was performed in a sham-operated group of rats except that the suture around the coronary artery was not tied. Isolation of total RNA was performed at 4 weeks after the onset of MI from noninfarcted myocardiums of resected LVs.

Statistics. Statistical analysis was performed using Mann-Whitney *U* test and single regression analysis. Data are presented as mean ± SEM. A *P* value less than 0.05 was considered significant.

Acknowledgments

We thank Ayako Hara (Core Technology Research Laboratories, Sankyo Co. Ltd.) for 5′-RACE analysis; Junichi Okutsu and Masatoshi Nishimura (Core Technology Research Laboratories, Sankyo Co. Ltd.) for microarray data analysis and critical reading of the manuscript; Tomoko Morita for technical assistance; Yulin Liao, Hidetoshi Okazaki, Hiroyuki Yamamoto, and Hisakazu Kato for thoughtful discussion; and A. Kawahara (Kyoto University) for establishing the zebrafish culture system. This study was supported by a grant from the Japan Cardiovascular Research Foundation; by Grants-in-aid for Human Genome, Tissue Engineering and Food Biotechnology (H13-Genome-011) and for Comprehensive Research on Aging and Health [H13-21 seiki (seikatsu)-23], both Health and Labour Sciences Research Grants from the Ministry of Health, Labor, and Welfare; by the Takeda Science Foundation; and by a Grant-in-aid for Scientific Research (no. 17390229) from the Ministry of Education, Science and Culture of Japan.

Received for publication October 31, 2006, and accepted in revised form June 26, 2007.

Address correspondence to: Seiji Takashima, Department of Cardiovascular Medicine, Health Care Center, Osaka University Graduate School of Medicine, 2-2 Yamadaoka, Suita, Osaka 565-0871, Japan. Phone: 011-816-8679-3472; Fax: 011-816-8679-3473; E-mail: takasima@medone.med.osaka-u.ac.jp.

1. Jessup, M., and Brozena, S. 2003. Heart failure. *N. Engl. J. Med.* **348**:2007–2018.
2. Kamisago, M., et al. 2000. Mutations in sarcomere protein genes as a cause of dilated cardiomyopathy. *N. Engl. J. Med.* **343**:1688–1696.
3. Olson, T.M., Michels, V.V., Thibodeau, S.N., Tai, Y.S., and Keating, M.T. 1998. Actin mutations in dilated cardiomyopathy, a heritable form of heart failure. *Science.* **280**:750–752.
4. Watkins, H., et al. 1995. Mutations in the cardiac myosin binding protein-C gene on chromosome 11 cause familial hypertrophic cardiomyopathy. *Nat. Genet.* **11**:434–437.
5. Collins, J.H. 2006. Myoinformatics report: myosin regulatory light chain paralogs in the human genome. *J. Muscle Res. Cell Motil.* **27**:69–74.
6. Chen, J., et al. 1998. Selective requirement of myosin light chain 2v in embryonic heart function. *J. Biol. Chem.* **273**:1252–1256.
7. Olsson, M.C., Patel, J.R., Fitzsimons, D.P., Walker, J.W., and Moss, R.L. 2004. Basal myosin light chain phosphorylation is a determinant of Ca2+ sensitivity of force and activation dependence of the kinetics of myocardial force development. *Am. J. Physiol. Heart Circ. Physiol.* **287**:H2712–H2718.
8. Kamm, K.E., and Stull, J.T. 2001. Dedicated myosin light chain kinases with diverse cellular functions. *J. Biol. Chem.* **276**:4527–4530.
9. Davis, J.S., et al. 2001. The overall pattern of cardiac contraction depends on a spatial gradient of myosin regulatory light chain phosphorylation. *Cell.* **107**:631–641.
10. Zhi, G., et al. 2005. Myosin light chain kinase and myosin phosphorylation effect frequency-dependent potentiation of skeletal muscle contraction. *Proc. Natl. Acad. Sci. U. S. A.* **102**:17519–17524.
11. Lazar, V., and Garcia, J.G. 1999. A single human myosin light chain kinase gene (MLCK; MYLK). *Genomics.* **57**:256–267.
12. Ruppel, K.M., Uyeda, T.Q., and Spudich, J.A. 1994. Role of highly conserved lysine 130 of myosin motor domain. In vivo and in vitro characterization of site specifically mutated myosin. *J. Biol. Chem.* **269**:18773–18780.
13. Aoki, H., Sadoshima, J., and Izumo, S. 2000. Myosin light chain kinase mediates sarcomere organization during cardiac hypertrophy in vitro. *Nat. Med.* **6**:183–188.
14. Kawakami, K., et al. 2004. A transposon-mediated gene trap approach identifies developmentally regulated genes in zebrafish. *Dev. Cell.* **7**:133–144.
15. Sharma, U.C., Pokharel, S., Evelo, C.T., and Maessen, J.G. 2005. A systematic review of large scale and heterogeneous gene array data in heart failure. *J. Mol. Cell. Cardiol.* **38**:425–432.
16. Herring, B.P., Dixon, S., and Gallagher, P.J. 2000. Smooth muscle myosin light chain kinase expression in cardiac and skeletal muscle. *Am. J. Physiol. Cell Physiol.* **279**:C1656–C1664.
17. Sehnert, A.J., et al. 2002. Cardiac troponin T is essential in sarcomere assembly and cardiac contractility. *Nat. Genet.* **31**:106–110.
18. Bar, H., et al. 2005. Severe muscle disease-causing desmin mutations interfere with in vitro filament assembly at distinct stages. *Proc. Natl. Acad. Sci. U. S. A.* **102**:15099–15104.
19. Ehler, E., Rothen, B.M., Hammerle, S.P., Komiyama, M., and Perriard, J.C. 1999. Myofibrillogenesis in the developing chicken heart: assembly of Z-disk, M-line and the thick filaments. *J. Cell Sci.* **112**:1529–1539.
20. Schonberger, J., et al. 2005. Mutation in the transcriptional coactivator EYA4 causes dilated cardiomyopathy and sensorineural hearing loss. *Nat. Genet.* **37**:418–422.
21. Ebert, A.M., et al. 2005. Calcium extrusion is critical for cardiac morphogenesis and rhythm in embryonic zebrafish hearts. *Proc. Natl. Acad. Sci. U. S. A.* **102**:17705–17710.
22. Davis, J.S., Satorius, C.L., and Epstein, N.D. 2002. Kinetic effects of myosin regulatory light chain phosphorylation on skeletal muscle contraction. *Biophys. J.* **83**:359–370.
23. Dias, F.A., et al. 2006. The effect of myosin regulatory light chain phosphorylation on the frequency-dependent regulation of cardiac function. *J. Mol. Cell. Cardiol.* **41**:330–339.
24. Rottbauer, W., et al. 2006. Cardiac myosin light chain-2: a novel essential component of thick-myofilament assembly and contractility of the heart. *Circ. Res.* **99**:323–331.
25. Schaper, J., et al. 1991. Impairment of the myocardial ultrastructure and changes of the cytoskeleton in dilated cardiomyopathy. *Circulation.* **83**:504–514.
26. Hein, S., Kostin, S., Heling, A., Maeno, Y., and Schaper, J. 2000. The role of the cytoskeleton in heart failure. *Cardiovasc. Res.* **45**:273–278.
27. van der Velden, J., et al. 2003. The effect of myosin light chain 2 dephosphorylation on Ca2+ -sensitivity of force is enhanced in failing human hearts. *Cardiovasc. Res.* **57**:505–514.
28. Margossian, S.S., et al. 1992. Light chain 2 profile and activity of human ventricular myosin during dilated cardiomyopathy. Identification of a causal agent for impaired myocardial function. *Circulation.* **85**:1720–1733.
29. Wakeno, M., et al. 2006. Long-term stimulation of adenosine A2b receptors begun after myocardial infarction prevents cardiac remodeling in rats. *Circulation.* **114**:1923–1932.

Circ J 2007; **71**: 289–293

Relationship Between Acute Rejection and Cyclosporine or Mycophenolic Acid Levels in Japanese Heart Transplantation

Kyoichi Wada, BS; Mitsutaka Takada, PhD**; Takashi Ueda, BS†; Hiroyuki Ochi, BS; Takeshi Kotake, PhD; Hideki Morishita, BS; Akihisa Hanatani, MD*; Takeshi Nakatani, MD*

Background Cyclosporine (CsA), Mycophenolate mofetil (MMF) and prednisolone (PSL) are widely used for the prevention of acute rejection after heart transplantation. Recently, the serum concentration–time curves (AUC) of CsA and MMF have been demonstrated to be precise predictors of acute rejection.

Methods and Results Fourteen heart transplant patients were treated concomitantly with CsA, MMF, and PSL between May 1999 and November 2005 at the National Cardiovascular Center and of them 3 had acute rejection episodes [International Society for Heart & Lung Transplantation grade 3a]. Two patients (man in his 30s; woman in her 40s) had acute rejection with a mycophenolic acid (MPA) $AUC_{0\text{-}12h}$ <30 $\mu g \cdot h \cdot ml^{-1}$ and low CsA AUC ($AUC_{0\text{-}4h}$; 2,408 $ng \cdot h \cdot ml^{-1}$, 1,735 $ng \cdot h \cdot ml^{-1}$). However, 1 patient (man in his 30s) with a high CsA $AUC_{0\text{-}4h}$ (4,019 $ng \cdot h \cdot ml^{-1}$) did not develop cardiac allograft rejection even if the MMF was temporarily stopped. These 3 patients were investigated to evaluate the relationship between acute rejection and pharmacokinetic parameters, including the CsA C_0, C_2, $AUC_{0\text{-}4h}$ and MPA $AUC_{0\text{-}12h}$.

Conclusions The findings suggest that a high CsA $AUC_{0\text{-}4h}$ may prevent rejection of a cardiac allograft, even if MMF is stopped or drastically reduced. (*Circ J* 2007; **71**: 289–293)

Key Words: Cyclosporine; Japanese heart transplantation; Mycophenolate mofetil; Serum concentration–time curve

A 3-drug combination therapy consisting of cyclosporine (CsA) or tacrolimus (FK) plus mycophenolate mofetil (MMF) and prednisolone (PSL) is commonly used for basic immunotherapy in heart transplant patients. At the National Cardiovascular Center (NCVC), approximately 30 heart transplant patients, including several from overseas, have received the 3-drug combination therapy, and its usefulness has been recognized[1,2] However, despite this treatment, some patients develop acute rejection. It is well known that, in order to obtain good clinical effects and to prevent acute rejection, it is important to monitor the blood levels of immunosuppressive agents. Generally, the trough level (C_0) has been used in such monitoring; however, in recent times, analysis of the full area under the curve (AUC) of CsA was demonstrated to be a precise predictor of acute rejection and graft survival[3] In addition, it was reported that in renal transplant patients, the AUC during the absorption phase ($AUC_{0\text{-}4h}$) was highly correlated with the full AUC and was a better marker for rejection and nephrotoxicity than the blood trough level[4] It has therefore come to be recognized that absorption profiling is needed in order to monitor the CsA microemulsion (Neoral) more effectively[4–11]

After oral administration, MMF is rapidly and extensively absorbed and hydrolyzed to mycophenolic acid (MPA), the active immunosuppressive agent. Several studies have demonstrated a significant relationship between the MPA AUC and acute rejection[12–19] A low AUC in the first 6 months is associated with a high incidence of rejection[13] and recent reports suggest that a target of 30–60 $ng \cdot h \cdot ml^{-1}$ may be suitable during both the early post transplant period and later for maintenance therapy in heart transplant patients[13,14,18,19]

We present 3 Japanese heart transplant recipients who showed a correlation between the development of acute rejection and the relevant pharmacokinetic parameters, including the CsA $AUC_{0\text{-}4h}$, the 2h post-dose concentration (C_2) and the MPA $AUC_{0\text{-}12h}$.

Methods

Of 14 patients who had received the 3-drug combination therapy between May 1999 and November 2005, 3 had acute rejection episodes (International Society for Heart & Lung Transplantation (ISHLT) grade 3a). In 2 of them, blood levels of CsA and MMF were measured before and after the acute rejection episode. Among the remaining 11 patients who did not have acute rejection episodes, 1 patient stopped the MMF for a long period and only received a 2-drug therapy (CsA and PSL). The 2 patients who had acute rejection episodes and the 1 who did not have an acute rejection episode during withdrawal of MMF were enrolled.

(Received October 11, 2006; revised manuscript received November 28, 2006; accepted December 11, 2006)

*Departments of Pharmacy, *Organ Transplantation, National Cardiovascular Center, Suita, **Division of Practical Pharmacy, Faculty of Pharmaceutical Sciences, Kinki University, Osakayama and †Department of Biochemistry and Molecular Biology, Kyoto Pharmaceutical University, Kyoto, Japan*

Mailing address: Kyoichi Wada, BS, Department of Pharmacy, National Cardiovascular Center, 5-7-1 Fujishirodai, Suita 565-0873, Japan. E-mail: kwada@hsp.ncvc.go.jp

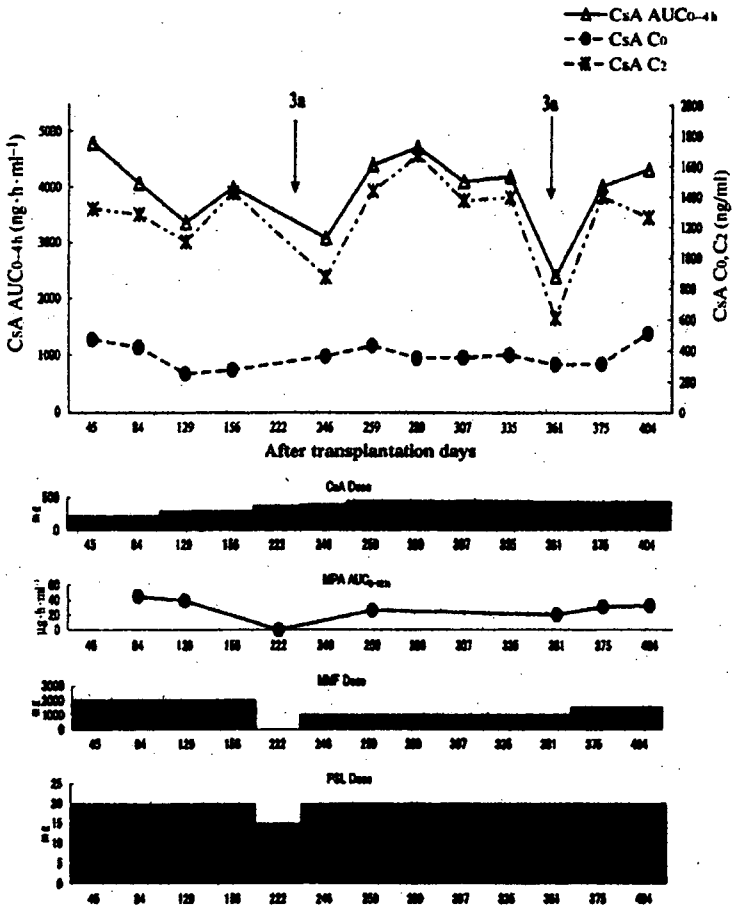

Fig 1. The blood concentration profiles of CsA and MPA, and the doses of CsA, MMF and PSL in patient 1. CsA, cyclosporine; AUC_{0-4}, area under the curve during the absorption phase; C_0, measurement of whole blood trough levels; C_2, 2 h post-dose concentration; MPA, mycophenolic acid; MMF, mycophenolate mofetil; PSL, prednisolone.

Blood for calculating the AUC of CsA and MPA was sampled at 6 time points: before dosing and at 1, 2, 4, 6, and 12 h after dosing. Blood levels of CsA and MPA were measured by fluorescent polarization immunoassay (TDx, Abbott Japan Co, Ltd) and reverse-phase high-perfomance liquid chromatography;[20] respectively. AUC was calculated using the trapezoidal method. The AUC_{0-4h} was calculated as:

$$AUC_{0-4h}=1/2\times\{(C_0+C_1)\times1\}+1/2\times\{(C_1+C_2)\times1\}+1/2\times\{(C_2+C_4)\times2\}$$

where C_1 is the 1 h post-dose concentration and C_4 is the 4 h post-dose concentration. All research procedures were conducted according to the institutional clinical research guidelines and all patients gave written informed consent concerning the disclosure of their clinical data.

Results

Patient 1 (Acute Rejection)

A man in his 30s man with dilated cardiomyopathy (DCM) as the underlying disease received a heart transplant under catecholamine treatment. At the time of transplantation, Human Leukocyte Antigen (HLA) (A, B, DR) compatibility was 0/6; cytomegalovirus (CMV) was (+) for the donor and (–) for the recipient. Initial immunosuppressive therapy was CsA, but the serum creatinine increased to 2.2 mg/dl, so CsA was discontinued from day 3 post-transplant and replaced with orthoclone-OKT3. After renal function improved, CsA was re-administrated with the addition of MMF and PSL.

The blood concentration profiles of CsA and MPA, and the doses of CsA, MMF and PSL are showed in Fig 1. The patient took oral ganciclovir (1,500 mg/day) to prevent CMV infection; however, on day 169 post-transplant, the CMV-polymerase chain reaction test showed a copy number of 1,900 and the antigenemia assay was positive. The patient was therefore hospitalized and ganciclovir injection therapy (10 mg·kg^{-1}·day^{-1}) was started.

The patient's leukocyte count decreased to 1,900/μl, which was an adverse reaction caused by ganciclovir and MMF. Therefore, both the ganciclovir injection and MMF (2 g/day) were stopped. The dose of CsA was increased from 300 to 360 mg. After that, on day 222 post-transplant, ISHLT grade 3a acute rejection was confirmed by myocardial biopsy. The CsA dose was 360 mg/day, MMF administration had ceased, and the dose of PSL was 15 mg/day. At this time, blood levels of CsA and MMF were not measured. Three-day pulse therapy with methyl prednisolone (MP, 1 g/day) was instituted, followed by an increase in the doses of CsA and PSL to 380 and 20 mg/day, respectively. MMF treatment was reinstated at 1 g/day. After 2 weeks, a myocardial biopsy showed improvement in the acute rejection, which was ISHLT grade 2. The target Co value of CsA was set at approximately 300 ng/ml.

On day 361 post-transplant, myocardial biopsy again revealed acute rejection of ISHLT grade 3a. The dose of CsA

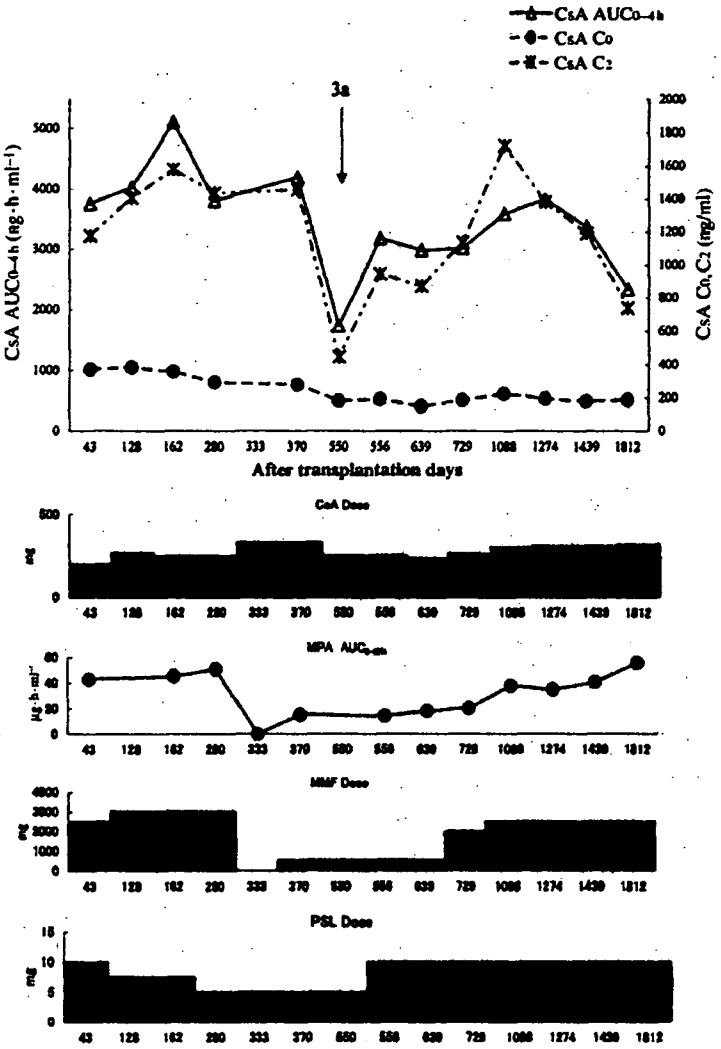

Fig 2. The blood concentration profiles of CsA and MPA, and the doses of CsA, MMF and PSL in patient 2.

was at 420 mg/day, C0 at 308 ng/ml, C2 at 607 ng/ml, and the AUC0-4h at 2,408 ng·h·ml^{-1}; the dose of MMF was 1 g/day, AUC0-12h of MPA was 20.8 μg·h·ml^{-1}, and the dose of PSL was at 20 mg/day. The grade of acute rejection improved following a 3-day course of pulse therapy with MP at 1 g/day. The C0 of CsA was at the target level with few variations, but despite that, acute rejection of ISHLT grade 3a occurred twice, and the patient sustained a pressure fracture of a vertebra because of PSL. In view of these findings, CsA was changed to FK.

Patient 2 (Acute Rejection)

A woman in her 40s with DCM as the underlying disease underwent cardiac transplantation after being on a NCVC extracorporeal left ventricular assist system (LVAS) (Toyobo, Tokyo, Japan)[21] HLA (A, B, DR) compatibility was 2/6, and CMV antibody was (+) for the donor and (+) for the recipient. At the time of the transplant, Panel Reactive Antibody was (–), as the cross-match test. Specific anti-HLA antibodies against the donor were found in the recipient. In addition, owing to concern about the possibility of a renal function disorder because of long-term use of the LVAS, immunosuppressive therapy was begun with OKT-3, then switched to the 3-drug combination therapy.

The blood concentration profiles of CsA and MPA, and the doses of CsA, MMF and PSL are shown in Fig 2. On day 333 post-transplant, the patient's leukocyte count had decreased to 3,400/μl, so MMF treatment (3 g/day) was stopped and the dose of CsA was increased from 280 to 330 mg/day. However, the serum creatinine level increased mildly to 1.3 mg/dl. On day 370 post-transplant, MMF treatment was reinstated at 0.5 g/day. CsA was maintained at 330 mg/day. The C0 of CsA was at 275 ng/ml, C2 at 1,452 ng/ml, and AUC0-4h at 4,204 ng·h·ml^{-1}. In addition, the AUC0-12h of MPA was 15.3 μg·h·ml^{-1}. subsequently, the serum creatinine level increased to 1.1 mg/dl and the CsA dose was decreased from 330 to 250 mg/day in order to obtain a target C0 of CsA of ≈200 ng/ml. On day 550 post-transplant, a myocardial biopsy was performed and acute rejection of ISHLT grade 3a was identified. At this point C0 was at 182 ng/ml, C2 at 445 ng/ml, AUC0-4h at 1,735 ng·h·ml^{-1}, the dose of MMF was 0.5 g/day, and that of PSL was 5 mg/day. Blood MPA level was not measured. After a 3-day course of pulse therapy with MP 1 g/day, the PSL dose was increased to 10 mg/day and acute rejection improved on day 556 post-transplant. The patient's leuko-

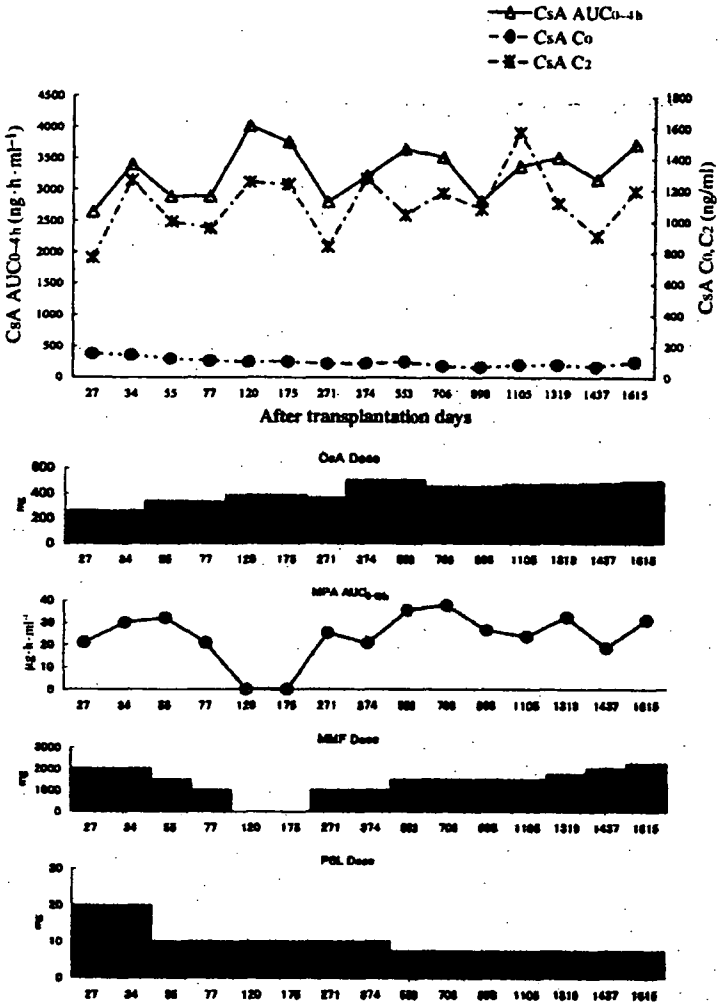

Fig 3. The blood concentration profiles of CsA and MPA, and the doses of CsA, MMF and PSL in patient 3.

cyte count recovered to the normal value, so MMF was gradually increased to 2.5 g/day. Thereafter, the dose of CsA was set according to the monitoring of C_2 and AUC_{0-4h}, and no further episodes of acute rejection occurred.

Patient 3 (Without Acute Rejection)

A man in his 30s with DCM as the underlying disease, underwent cardiac transplantation under the support of LVAS. HLA (A, B, DR) compatibility was 0/6, CMV antibody was donor (+) and recipient (+). After the transplant, the patient's serum creatinine level increased to 2.2 mg/dl so immunosuppressive therapy was initiated with OKT-3, followed by the 3-drug combination therapy.

The blood concentration profiles of CsA and MPA, and the doses of CsA, MMF and PSL are showed in Fig 3. Up to day 75 post-transplant, the MMF dose was at 1.5 g/day, but the leukocyte count decreased to 3,770/μl, so the MMF dose was decreased from 1.5 to 1 g/day. On day 99 post-transplant, the leukocyte count decreased further to 3,270/μl, MMF was stopped and the CsA dose was increased from 320 to 380 mg/day. When the CsA dose was at 320 mg/day, C_0 was at 267 ng/ml, C_2 at 954 ng/ml, and AUC_{0-4h} at 2,897 ng·h·ml^{-1}. When the CsA dose was at 380 mg/day, C_0 was at 247 ng/ml, C_2 at 1,249 ng/ml, and AUC_{0-4h} at 4,019 ng·h·ml^{-1}. On day 262 post-transplant, the leukocyte count recovered to 8,000/μl, which is within the normal range, so MMF treatment was reinstated at 0.5 g/day. During the washout of MMF, myocardial biopsy was performed twice, but acute rejection was not seen.

Discussion

Our experience with the 3 heart transplant patients presented here suggests that monitoring of the CsA AUC_{0-4h} or C_2 may be useful in preventing acute rejection, as may a high AUC_{0-4h} or C_2, even if MMF is stopped or drastically decreased.

In patient 1, the CsA AUC_{0-4h} and C_2 were greatly decreased, with a low MPA AUC_{0-12h} (20.8 ng·h·ml^{-1}) on day 361 post-transplant (ISHLT grade 3a). In patient 2, the CsA AUC_{0-4h} and C_2 greatly decreased on day 550 post-transplant (ISHLT grade 3a). Although the MPA AUC_{0-12h} value on day 550 was not calculated, approximately 15 ng·h·ml^{-1} could be predicted because the MPA AUC_{0-12h} values on days 370 and 556 were 15.3 μg·h·ml^{-1} and 14.3 μg·h·ml^{-1}, respectively. The MPA dose remained unchanged from day 370 to day 556. Low CsA AUC_{0-4h} and MPA AUC_{0-12h} might have been the cause of acute rejection on